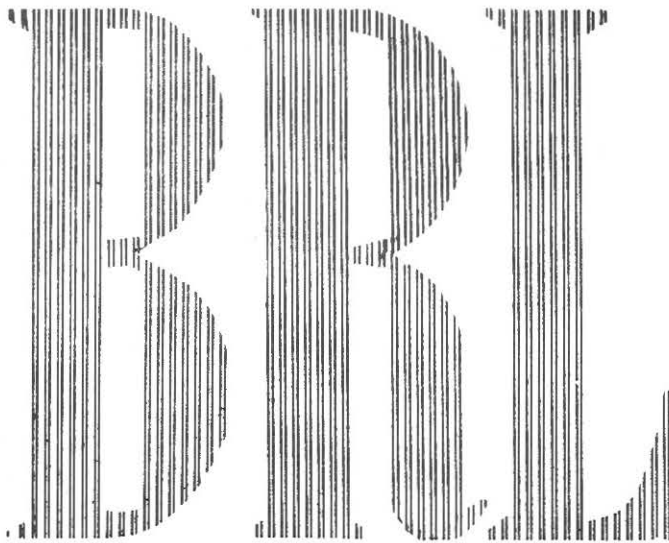


Robert L Mc Coy

AD 200177



REPORT NO. 1044

JUNE 1958

## THE TRANSONIC FREE FLIGHT RANGE

WALTER K. ROGERS, JR.

DEPARTMENT OF THE ARMY PROJECT NO. 5B03-03-001  
ORDNANCE RESEARCH AND DEVELOPMENT PROJECT NO. TB3-0108  
**BALLISTIC RESEARCH LABORATORIES**



**ABERDEEN PROVING GROUND, MARYLAND**

BALLISTIC RESEARCH LABORATORIES

REPORT NO. 1044

JUNE 1958

THE TRANSONIC FREE FLIGHT RANGE

Walter K. Rogers, Jr.

Department of the Army Project No. 5B03-03-001  
Ordnance Research and Development Project No. TB3-0108

ABERDEEN PROVING GROUND, MARYLAND

## PREFACE

The present report is a revised edition of BRL Report 849 entitled The Transonic Free Flight Range<sup>1</sup>. At the time that the first edition was published, the range had been in operation for only three years. At present, after eight years of operation, there have been substantial improvements in both instrumentation and techniques. Moreover, the increasing variety of configurations that are being fired through the range demonstrate its flexibility as an aerodynamic tool. Thus it was felt that a revised edition of the original report was needed.

BALLISTIC RESEARCH LABORATORIES

REPORT NO. 1044

WKRogers/cr  
Aberdeen Proving Ground, Md.  
June 1958

THE TRANSONIC FREE FLIGHT RANGE

ABSTRACT

This report contains a current description of the Transonic Free Flight Range. This range, developed at the Ballistic Research Laboratories at Aberdeen Proving Ground for ballistic and aerodynamic research, has been in operation for approximately eight years. The accuracy and reliability of the results obtained from this range make it a valuable tool for the free flight testing of missiles and for research in compressible flow phenomena.

The range, its instrumentation, and the experimental procedures associated with their use are described. The various records obtained in the range and an indication of the method employed in the reduction of the raw data into final aerodynamic coefficients are also described.

In an appendix is an outline of the steps and reasoning behind the design of the Transonic Range.

There is a listing of selected references to similar reports on other free flight ranges, and on the reduction, capabilities, and use of free flight range data.

## TABLE OF CONTENTS

1. INTRODUCTION . . . . .	9
2. DESCRIPTION OF THE FACILITY. . . . .	11
3. PREPARATION FOR AND FIRING OF A PROGRAM. . . . .	18
4. RECORDS PRODUCED BY THE RANGE. . . . .	20
5. REDUCTION PROCEDURE. . . . .	22
6. ACCURACY . . . . .	26
6.1 Class I . . . . .	27
6.2 Class II . . . . .	29
7. REPRESENTATIVE DATA. . . . .	29
8. REPRESENTATIVE PROGRAMS. . . . .	30
9. SUMMARY. . . . .	31
10. REFERENCES . . . . .	33
11. APPENDIX - Design of the Transonic Range . . . . .	35
12. FIGURES. . . . .	41
13. DISTRIBUTION LIST. . . . .	65

## 1. INTRODUCTION

The Transonic Range of the Ballistic Research Laboratories is part of the Free Flight Aerodynamics Branch of the Exterior Ballistics Laboratory. Missiles traveling through this enclosed spark photography range are not restrained or affected by any forces other than those normally encountered in flight.

The purposes of this range are threefold:

1. To provide data for determining the aerodynamic coefficients of projectiles up to 8 inches in diameter or wing span.
2. To provide an accurate instrument with which to investigate the causes of dispersion of projectiles.
3. To provide data on flow characteristics from the subsonic through the transonic and on into the higher regions of velocity.

The Transonic Range has many predecessors and contemporaries as a free flight range. The first such range is believed to have been built at the National Physical Laboratory in England. The second range was built and used in this country by Dr. R. H. Kent at Aberdeen. Along the same lines as Dr. Kent's range, was the Free Flight Aerodynamics Range<sup>2</sup> built at the Ballistic Research Laboratories under the direction of Dr. A. C. Charters. Dr. Charters was largely responsible for the instrumentation of this range. Dr. Charters, Dr. E. M. Little, and Mr. R. L. Rowe were responsible for the major part of the design and building of the Transonic Range.

There are a number of contemporary ranges in North America such as:

1. A pressurized range at BRL, Aberdeen Proving Ground, Maryland<sup>3</sup>.
2. Two ranges, one of which is pressurized, at Naval Ordnance Laboratory at Silver Spring, Maryland<sup>4</sup>.
3. A large range at Naval Ordnance Test Station at China Lake, California<sup>5,6</sup>.
4. A range and wind tunnel combination at the Ames Aeronautical Laboratory of the NACA, Moffett Field, California<sup>7,8</sup>.

5. A large range at Canadian Armament Research and Development Establishment, near Quebec City<sup>9</sup>.

In free flight ranges the usual ballistics problem is worked in reverse. Usually one obtains aerodynamic coefficients from a wind tunnel, calculates them from theory, or makes estimates from previous experience or data available on similar shapes. Having this information and using ballistic theory, one calculates the motions and trajectory of the missile. However, in the free flight method, one observes the motions of the projectile and with proper ballistic theory, calculates the aerodynamic forces and moments that would have been necessary to produce such a motion.

## 2. DESCRIPTION OF THE TRANSONIC RANGE FACILITY

The Transonic Range was designed in 1944 and primary construction completed in 1947. The instrumentation was completed for full scale operation in the summer of 1950.



FIGURE 1

The range, shown in Figure 1, is 1173 feet long. The part of the building nearest the gun position is reinforced concrete while the remainder is sheet metal on a steel frame. The first 750 feet of the range is 24 x 24 feet in cross section and is fully instrumented. The remaining 423 feet, which was added in recent years has never been instrumented but does facilitate extension of roll histories



through the use of yaw card techniques. The metal sections of the building are insulated and have an aluminum covering. The instrumented section has radiant heating.

The projectile to be tested is usually launched from a gun. It passes through the opening in the large concrete blast shield and then into the enclosed range.

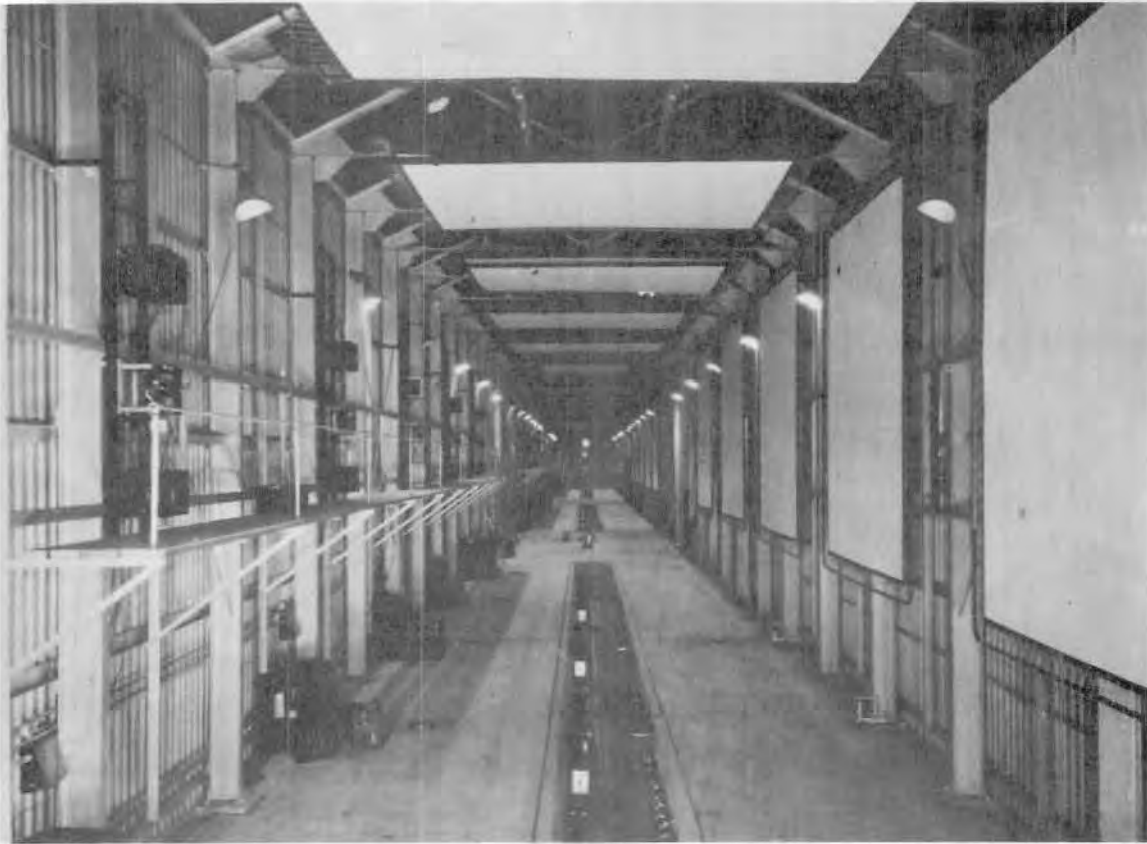
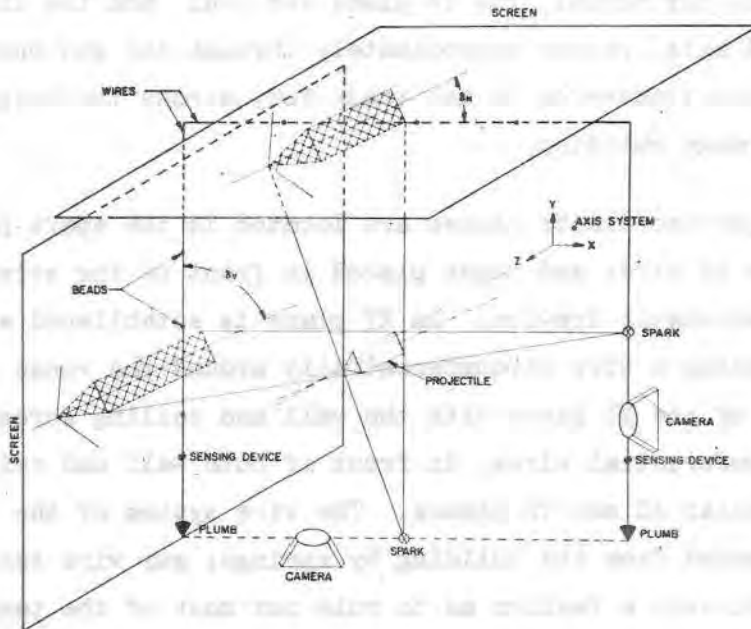


FIGURE 2

Figure 2, a photograph of the interior of the Transonic Range, shows 15 of the full complement of 25 spark photographic stations arranged in five groups of five stations each. These stations each furnish a tiny chapter in the motion history of the model's passage through the range. The apparatus will be described in detail in the following paragraphs.

In order to illustrate the instrumentation within the range building, a schematic drawing of the set-up is presented in Figure 3.

FIG.3 SCHEMATIC DRAWING OF INSTRUMENTATION SET-UP IN RANGE



The projectile, as located in space, is seen at the center with spark generator and camera combinations on the right and bottom. A close view of a spark generator and a camera in a pit is seen in Figure A4\*.

The sparks are generated in confined air gaps of the Libessart type which approximate a point source. A picture of the mechanism is found in Figure A5. The voltage used is 15 KV and capacitance 0.25 microfarad. These sparks project shadows of the projectile and the surrounding flow phenomena upon the large beaded screens

\* Hereafter Figure numbers preceded by capital letter A will indicate illustrations in the section under "FIGURES", pp41.

seen at the left and top of Figure 3. The cameras take pictures of the shadows projected on these screens. The cameras are equipped with  $f/2.5$ , 7 inch focal length lenses.

In order to locate the projectile in space a rectilinear coordinate system has been established throughout the range. The coordinate axes are: X, horizontal and normal to the line of fire; Y, vertical; and Z, horizontal and along the line of fire. Consequently, the XZ plane is horizontal, the YZ plane vertical, and the intersection of both, the Z axis, passes approximately through the gun muzzle. The XY plane extends transverse to the trajectory across the height and width of the range building.

These major coordinate planes are located in the spark photographs by the shadows of wires and beads placed in front of the screens as shown in the schematic drawing. An XY plane is established at each station by placing a wire circumferentially around the range along the intersections of the XY plane with the wall and ceiling screens. Beads on these circumferential wires, in front of both wall and ceiling screens, establish XZ and YZ planes. The wire system of the vertical walls is suspended from the building by springs; guy wire tents anchor the position in such a fashion as to rule out most of the temperature movements of the building itself. Sensing devices, as seen in the schematic drawing, are installed to sense any movement in six directions of freedom so that corrections can be made before firing. The vertical and horizontal spark gaps are placed in this same XY plane.

A careful survey is required\* to place the fiducial wires. The XZ plane is determined with a precision level. The YZ plane is determined by stretching a wire the entire length of the range and projecting the resulting line down upon secondary bench marks secured in the floor as seen in Figure A6. These bench marks also locate the XY plane. Their

---

\* The primary ideas for these survey methods were furnished by Mr. Robert L. Rowe of the Free Flight Aerodynamics Branch.

distance along the range is measured with great accuracy by a precision tape survey. The spark gaps and cameras are elevated in an XY plane by means of a precision theodolite. See Figure A7.

Additional features seen in Figure 2 are the photoelectric screens placed along the trajectory, one ahead of each station. These may be seen in close-up in Figures A8 and A9. These screens consist of a light source, a cylindrical lens to fan the light out into a sheet, a reflective screen strip, and another cylindrical lens which focuses the returning light onto the filament of a photo multiplier tube. The passage of the projectile interrupts the sheets of light causing a signal from the photocell. This signal is amplified, delayed, and then used to trigger the dual spark gaps of the station at the instant the projectile is opposite the approximate center of the screen. These photoelectric screens have proven very successful and are sensitive enough to be triggered by 20-mm projectiles.

It might also be noted, that in Figure 2 there are two spark sources and one camera on the wall of the range. This arrangement was made to cover a wide variety of trajectory variations in the vertical plane. At times both of these vertical sources are used, one being synchronized with the spark in the other plane and the second delayed slightly. The resulting shadowgraph is double and allows, at least in one plane, the study of projectiles with short oscillatory periods. In the immediate future second spark sources will be placed within the pits and along the walls to further implement this type of study. Figure A10 shows an example of this dual exposure. The same fiducial system is used for both shadows. The fiducial wire with reference beads as well as the tent wires for holding tension on the spring suspension system, may be seen. The two blurred images are photographs of the projectile itself, not its shadow.

The equipment on the floor of the range was put into pits for protection and convenience. The primary stations within each group are 20 feet apart with a 70 foot interval between groups. Thus, between the first station and the last there are 680 feet.

In Figure A11 another type of station set-up, used in the Transonic Range, is illustrated. This apparatus is for taking a direct photograph of a projectile in flight. This method is not always successful toward the exit end of the range where greater dispersion causes the depth of field to be large. The direct photography method, however, is especially useful as auxiliary instrumentation to show the external condition of fins, rotating bands and other parts most subject to launching damage. A microflash photograph may be seen in Figure A12.

To study causes of dispersion of projectiles one would like to know: the motion of the projectile in the launcher; any reaction between the launcher and the projectile before and during emergence; the reaction of the projectile in the muzzle region or while it is affected by muzzle gases; and last, a timed history of projectile motion until some target or measure of dispersion is reached at the conclusion of its recorded flight.

The Transonic Range offers high-speed motion picture coverage and other techniques which satisfy the majority of the launching requirements, and the enclosed range instrumentation which completes the package of initial conditions of launch. A fairly well instrumented target area terminating at 1000 yards from the launching ramp completes the picture.

The third purpose of the range, to provide data on detailed flow characteristics, is partially satisfied by the regular spark records. However, another piece of specialized instrumentation has been developed to further this purpose. It is called a mosaic. As this name indicates, it consists of a series of large 11" x 14" photographic plates laid out together on a table top placed just below the calculated trajectory. A spark source, located above these plates is triggered in the same way as the standard stations and the large mosaic picture is obtained. This picture shows flow detail in such a size as to be easily studied for small effects. When trajectories can be closely estimated then the distance from spark to plates in this set-up can be shortened to perhaps



as little as five feet. This allows the use of a fast and less intense spark and results in sharper detail than the usual shadow station already described. A photograph of one of these mosaic tables is seen in Figure A13; a mosaic picture in Figure A14.



FIGURE 15

The instrument building, located some 1000 feet from the range itself, is shown in Figure 15. It contains offices, photographic dark rooms, a model and instrument shop, an electronics laboratory, and a physical measurements laboratory which serves both this large range and the smaller Aerodynamics Range. This latter laboratory furnishes measurements of the physical properties of models such as dimensions, moments of inertia, center of gravity positions and other pertinent characteristics. The work is described in Reference 11. The chronograph counters, previously located in the instrument building, have recently been put into operation in a new instrument shelter (Figure A16) which is located just outside the range itself. This shelter eliminates long signal cables to the instrument building and is more efficient for housing personnel during actual firing. The shelter contains 1.6 megacycle

counters (Figure A17) with an accuracy of approximately  $5/8$  microsecond. The pulses to the counters are received over coaxial cables from the range spark stations. Figure A17 also shows a control console which is used to operate cameras, bias control, and round-numbering devices on the cameras. The range personnel operate a temperature controlled loading and storage room (Figure A18) where propellants are carefully measured and stored under constant temperature prior to firing programs. A magazine for storage of supplies of propellant and some projectiles awaiting test is within the facility area but is not shown.

Associated with the Free Flight Aerodynamics Branch are three model shops - one at the Transonic Range, one in the main Ballistic Research Laboratories' building and one in the Wind Tunnel building. These shops manufacture most of the models for research and, in some cases, models for contracting agencies or parts of experimental service rounds.

### 3. PREPARATION FOR AND FIRING OF A PROGRAM

The above general description of the range facilities will be expanded below as it applies to the actual preparation for and firing of a program at the Transonic Range.

The model shops, after receiving the approved designs for projectiles, manufacture the models. Employed in the model making are the usual precision toolmakers' tools with a few special purpose instruments such as an air tracer attachment for the lathes which automatically follows pre-ground templates of missile contour and a precision contour grinder with an accuracy of  $\pm .0003''$ , for use in grinding these model contour templates.

After the models are manufactured, they are taken to the physical measurements laboratory for measurements. The moments of inertia, both transverse and axial, are determined on a torsion pendulum by comparison with known test masses. The periods are measured by means of electronic timing. The timing signal is produced and recorded through a photo-cell

optical-counter combination. A 105-mm shell is shown in a torsion pendulum in Figure A19.

While the manufacture and measurements are being completed, the means of launching must be determined. To date all launchings, with the exception of some rockets, have been made from breech loading guns. Some projectiles, because of external configuration, desired initial angle of launch, maximum pressure limits, required spin, and protection of surface finish may require special individual launching devices. These devices are usually called sabots<sup>12</sup>. Their purpose is to assure desirable launching conditions, and sufficient obturation of propellant pressures for the required velocity and successful flight into and through the enclosed range. Each sabot is designed to fit the particular set of launching conditions and the type of projectile.

The expected trajectory or flight path is calculated by standard methods and the optimum spark height is selected to best fit this path. As previously mentioned, each spark unit contains a delay system which must be adjusted to the expected velocity to allow the projectile to proceed to a point opposite the center of the reflective screen before the spark is discharged.

After all of the above preparations have been made, a systematic firing procedure is carried out. The cameras are loaded with photographic plates and the Fastax high-speed motion picture cameras with film. All personnel are cleared from the possible danger areas. The projectile and propellant are loaded into the gun. From the instrument shelter, the round number and station designation are exposed on the plates, the cameras are opened and a bias control operated which allows the spark stations to operate on the pulse from the photocell trigger units. The gun is fired, cameras are closed and the range personnel collect the plates for processing in the photographic dark room.



#### 4. RECORDS PRODUCED BY THE RANGE

The basic records obtained in the Transonic Range are the spark shadowgraphs on 4" x 5" photographic plates, a print of which is presented in Figure 20.

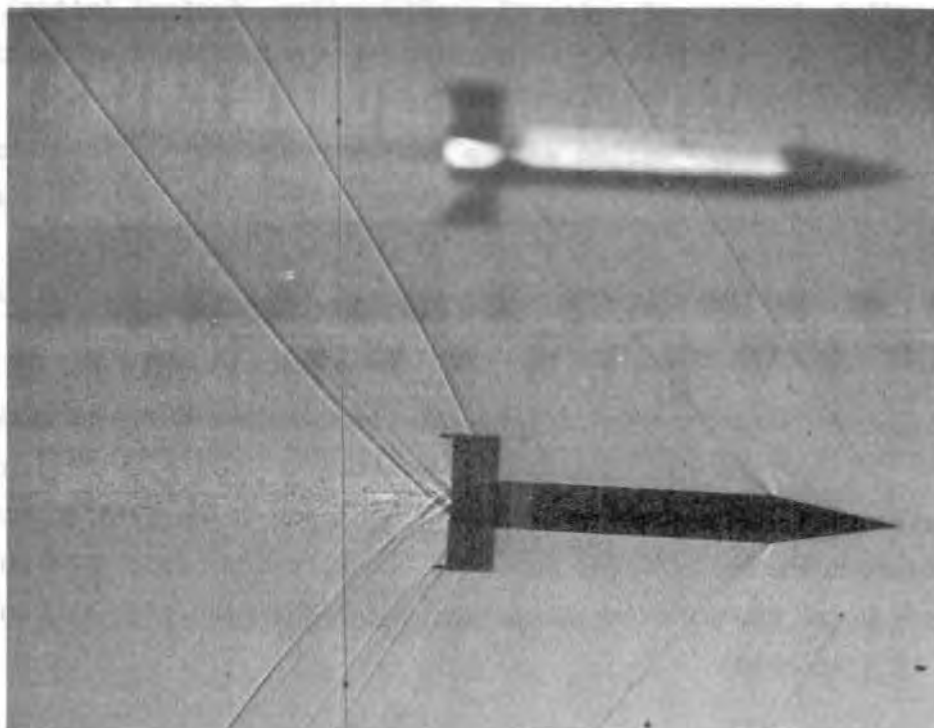


FIGURE 20 - Shadowgraph - Finned Cone Cylinder  
(6-inch fin span) Pitch Model

Velocity - Approximately 1400 ft/sec  
Mach. No.- Approximately 1.2

As mentioned before the blurred image is the projectile itself. The sharp, black silhouette with the attached flow phenomena is the shadow of the projectile on the screen. The appearance of the flow phenomena in a shadowgraph such as Figure 20 might be explained in the following manner: the intensity, at the reflective screen, of the light which passed through the air around the projectile is a function of the density variation in the air. The density gradient in the disturbed flow causes a deflection of the light rays in the direction of the gradient. This refraction of the light causes a dark line or lessening of the light intensity at the front

of the shock wave and a light line or buildup of light at the rear of the wave. The shadows of the fiducial wires and beads which define the coordinate planes can be seen. Other examples are shown in Figures A21, A22, A23, A24, and A25.

The second type of record is the direct photograph or microflash picture. Examples of this type are Figures A12 and A26, previously described. In both examples there is a spiral painted on the ogive of the projectile. Measurements of this spiral, on a succession of microflash pictures taken at appropriately spaced stations, result in a reasonably accurate determination of axial spin rate. These pictures show no flow phenomena but are very valuable for determining possible launching damage to missiles.

Another type of photographic record, previously discussed and illustrated, is the large mosaic or multi-shadowgraph.

A fourth type of record is the film from Fastax high-speed motion picture cameras which gives a history of the launching between the muzzle and the enclosed range. This record is not only very important for dispersion studies of military weapons but imperative for the design and testing of the launching devices (sabots) for airplanes, bombs, and missiles. An example of a record of a 16-mm framing camera, capable of speeds up to 15,000 frames/second, is given in Figure A27. An example of a record of a "smear" type of camera is presented in Figure A28. In this type, the rotating prism is removed from the framing camera and replaced by a slit. The film is then run at the same speed and direction as the image of the projectile. The image then is "smeared" through the slit onto the film. The resulting photograph is a single picture, usually excellent in detail and clarity.

In addition to photographic records, time and meteorological records are obtained. Time intervals are indicated in the counters, then read and recorded by range personnel. At present, fifteen stations are wired to send timing signals. The barometric pressure, temperature, and relative humidity of the range atmosphere are also recorded.

## 5. REDUCTION PROCEDURE

The range records are processed by the Data Reduction Section to determine those aerodynamic forces and moments which are related to the motions of the missile as observed in the photographs. As has been previously described, the photographs contain shadows of fiducial wires and beads to form a YZ reference system on the wall or vertical plate and an XZ reference on the floor or horizontal plate. These plates are placed on an optical comparator\*. It is possible to locate some point on the projectile and measure its distance from the reference wire and bead. See Figure A30 for plots of X and Y versus Z of a representative example. The angles of inclination of the missile's axis to the wire also are recorded. Now, knowing both the physical properties of the projectile and the geometry of the range, the position of the center of gravity and the inclination of the axis in space are determined.

Throughout the last twenty to thirty years the theories of the yawing motion of a projectile in free flight have been developed by R. H. Fowler, E. G. Gallop, C. N. H. Lock, H. W. Richmond, R. H. Kent, J. L. Kelley, E. J. McShane, F. Reno, and others. Up-to-date application of these theories to the reduction of data from a free flight range was further refined by the use of high speed computing machines<sup>13</sup>. Applications of these theories for the analysis of the motion of a large variety of configurations may be found in the reports listed in the references at the end of this paper.

Time and yaw are both continuous functions of distance along the range, but the values of these functions are controlled by the aerodynamic properties of the missile.

The drag coefficient,  $K_D$  (neglecting yaw effects), is easily determined. It has been found both theoretically and experimentally that over a short range, the time position of the projectile can be

---

\* The optical comparator (shown in Figure A29) gives a magnification of 6-9 and provides a linear measurement accuracy of .001 inch and an angular accuracy of one minute.

adequately expressed as a cubic polynomial in distance.

$$t = a_0 + a_1 (z - z_m) + a_2 (z - z_m)^2 + a_3 (z - z_m)^3$$

where

$t$  = observed time, seconds

$z - z_m$  = distance from mid-range ( $z_m$ ), feet

By the use of a least squares fit to the experimental observations, the coefficients in this equation may be determined.

The velocity and retardation at the center of the range are:

$$v = \frac{1}{a_1}, \quad \frac{dv}{dt} = \frac{-2a_2}{a_1^3}$$

The product of retardation and mass gives the drag force and the drag coefficient:

$$K_D = \frac{\text{drag force}}{\rho d^2 v^2} = \frac{m}{\rho d} \frac{2a_2}{a_1^3},$$

where

$\rho$  = air density in slugs

$d$  = diameter of projectile in feet

$v$  = velocity in ft/sec

$m$  = mass

With some models of very blunt, high-drag shape, the Mach number variation is rather large. The range instrumentation furnishes sufficient information so that the data may be broken into two or more sections and drag coefficients obtained from each.

The yawing motion for symmetric missiles can usually be approximated by a damped epicycle with slowly varying rates. See Figures A31 and A32 for examples of plotted epicycles from sample data. In order to handle the problem, the assumption is usually made that over a short distance

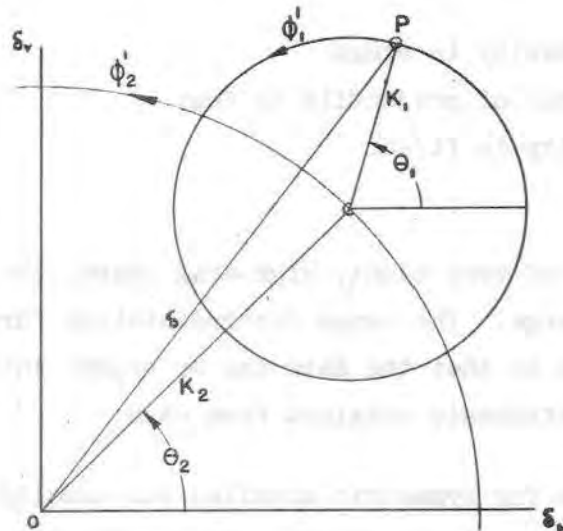
(namely, 80 feet in the Transonic Range) the damping of the arms of the epicycle and the variation of rates are negligible and the yaw of repose is neglected for a first approximation. This leads to the following type formula:

$$\delta_H + i\delta_V = \delta = K_1 e^{i\theta_1} e^{i\phi_1'} (z - z^*) + K_2 e^{i\theta_2} e^{i\phi_2'} (z - z^*)$$

where

- $\delta$  = yaw with respect to a tangent to the actual trajectory
- $K_1$  = nutational or fast rotating arm (outer arm)
- $K_2$  = precessional or slow rotating arm (inner arm)
- $\theta_{1,2}$  = phase angles of above arms
- $\phi_{1,2}$  = rotational rates of arms
- $z$  = distance down range
- $z^*$  = position of projectile at center station, within each group.

FIG. 33 GEOMETRICAL INTERPRETATION  
OF YAWING MOTION





To add some clarity to the above statements and formula, Figure 33 is presented to give a geometrical interpretation to the yawing motion. Since the pure epicyclic motion may be constructed of two circular motions, these are shown as the rotation of arm  $K_2$  about the origin at rate  $\phi_2'$  and rotation of  $K_1$  about the end of  $K_2$  arm at the rate  $\phi_1'$ . Thus, any point P on the outer or nutational circle is rotating about a center which is itself rotating about the origin.  $\theta_1$  and  $\theta_2$  are phase angles of the two radii at  $z^*$ .

A first approximation to the above equation may be obtained graphically. This is accomplished by assuming a series of values for the slow rate  $\phi_2'$  and by rotating the yaw vectors at these rates until the end points of these vectors lie in a circle. See Figure A34 for an example of a circle obtained from sample data. With the spark stations grouped as they are in the present range set-up, each group of five stations is used to determine one circle and there are five such circles for the complete range. From these individual circles, the parameters  $\phi_1'$ ,  $\phi_2'$ ,  $K_1$ ,  $K_2$ ,  $\theta_1$  and  $\theta_2$  are determined.

Having completed the first approximation of the unknowns involved in the yaw equation, the computer proceeds with the second approximation which takes into account damping rates. However, with the rough parameters gained from the first approximation he may proceed directly to the iterative method of differential corrections to these values. This work is usually carried out on one of the high speed computing machines in the Ballistic Research Laboratories and can be continued until the sum of the squares of the residuals is at a minimum. These differential corrections when added to the initial values give the final values of the desired parameters.

If the computer is successful with the approximations above, he may obtain  $K_M$  the moment coefficient, and  $K_A$  an estimate for the spin deceleration coefficient directly. A more accurate  $K_A$  can be had from a spin reduction, where possible. The lift coefficient,  $K_L$ , must be obtained from either a swerve reduction<sup>13</sup> or from the results of a

program in which the center of gravity of the projectiles is varied. Once  $K_L$  is determined and using parameters obtained in the yaw and drag reduction,  $K_H - K_{MA}$ , the damping moment coefficients, and  $K_T$ , the Magnus torque coefficient, may be obtained.

It is not the intent of this report to go further into the details of a reduction procedure. The reference reports are given for those wishing to go into complete methods and variations. The discussion above was, of course, for the simpler cases of missile motion. When aerodynamic asymmetries are present, the type of motion becomes a bit more difficult to handle and is termed "tricyclic" (as one might expect, a third arm is added, about which the other two arms rotate). The proven method of handling this motion can be found in references 14, 15, and 16. The theory is set forth in reference 13. The handling of aircraft models carries the asymmetry case to an extreme and reference 17 is given for those who might be interested.

It may be said that with the present method of reduction, the complete procedure for one round takes one computer approximately one week. Machine methods, however, are now being studied to reduce this time. A semi-automatic measuring machine to further reduce the time required for the laborious task of plate measuring is being evaluated.

The Laboratory has had in operation for some time a Goodyear Electronic Differential Analyser (GEDA) for study of nonlinear problems. References 18 and 19 discuss this machine. The measurement of nonlinear forces and moments, by means of free flight tests, is described in References 20 and 21.

## 6. ACCURACY

Errors in Transonic Range work might be divided into two classes. The first class includes those that are of a physical nature, while the second class includes the errors in the fit of the theories of yawing motion and drag to the experimental data obtained in the range. Both of these classes of errors are discussed below:

## 6.1 Class I

The physical errors are in the measurement of the missiles; the measurement of time, distance, temperature and pressure in the range; and the measurement of the photographic plates.

The estimated tolerances applied to the physical measurements of missiles are:

<u>Measurement</u>		<u>Tolerance</u>	<u>Means of Measurement</u>
dimensions	length	.002 in.	vernier calipers
	diameter	.001 in.	micrometers
weight		.02 lb	platform, no-spring scale
position of the center of gravity		.01 in.	special balance system
moments of inertia		.05 %	torsion pendulum
surface roughness		.00001 in.	profile recorder
angles		1. min.	optical protractor
wing or fin profile measurements			
	angle	1. min.	airfoil contour scribe
	length	.0005 in.	

A conservative estimate of the time error as measured by the electronic counters is  $1 \times 10^{-6}$  seconds. The distance measurements are made in the Transonic Range to an initial survey accuracy (repeatable) of better than  $1 \times 10^{-3}$  feet. The building is thoroughly insulated and has radiant heating in the floor so that accuracies hold for some time. Primary bench marks are mounted, independent of the building structure, on individual I beams which have been driven into the earth (See again Figure A6). The survey wire-and-bead system is so constructed that it is nearly independent of any building movements.

There are other errors in the distance measurement in the range which are involved in the spark photographic techniques. There is an error due to spark duration which shows movement of the projectile and results in blurring of the photograph. The spark at present has a



duration of about  $3 \times 10^{-6}$  seconds, which for a projectile velocity of 2000 ft/sec, would allow a projectile movement while being photographed of about 1/16 inch. There is also a possible error due to the two sparks at a station not being synchronized. This error would allow the projectile to move farther in one of the two pictures and give an inaccuracy in the final space coordinate of the center of gravity. From oscillograph measurements it is found that this error for the average double spark set-up is about  $3 \times 10^{-6}$  seconds, or again approximately 1/16 inch in space (projectile velocity again assumed to be 2000 ft/sec).

Errors in the determination of the air density in the range affect the values of the aerodynamic coefficients either directly or indirectly. In the evaluation of those coefficients in which the air density is a factor, percent errors in this quantity result in equal percent errors in the coefficient values.

The evaluation of the air density in the range is dependent on the pressure and temperature recorded in the range building. Round to round determination of air density indicates a 1/2% error in this quantity. Also, temperature gradients in the range of  $\pm 2^{\circ}$  cause the average absolute values of air density to be as much as 1/2% in error.

Evaluation of Mach number in the range is also affected by the magnitude of the temperature gradients. The error in Mach number is approximately half of the absolute density error as given above.

The accuracy with which the photographic plates can be read on the optical comparators is about  $1 \times 10^{-3}$  inches for position measurement and  $5 \times 10^{-2}$  degrees for angular measurement. The former error results in about 1/64 inch error in space position.

## 6.2 Class II

The most difficult error to define is the error of the fit of the theory to the experimental points. Since the physical errors, as discussed above, are already included in the experimental data, this error of fit is a measure of the overall accuracy of the theory and the range data. Disregarding a few unusual cases where the theories do not fit experiments too well, a magnitude for this total error can be given from experience with the range results. The maximum fitting error for the yawing motion is about  $1 \times 10^{-1}$  degrees and for the drag determination, a distance error of about  $1 \times 10^{-2}$  feet.

Experience with range results in the form of aerodynamic coefficients indicates the following magnitudes for errors:

<u>Coefficient</u>	<u>Estimated Error in Percent</u>
$K_D$ Drag ( $C_D$ )	1
$K_L$ Lift ( $C_{L\alpha}$ )	5
$K_M$ Moment ( $C_{m\alpha}$ )	2
$K_H - K_{MA}$ Damping Moment ( $C_{m\dot{q}} + C_{m\dot{\alpha}}$ )	15
$K_T$ Magnus Moment ( $C_{m_{p\alpha}}$ )	15

## 7. REPRESENTATIVE DATA

For reasons of classification a single full program will not be presented. Instead a series of illustrative graphs will be given. These data are indicative of what might be expected from range programs but should not be used otherwise.

1. In Figure A30 the x and y coordinates of the center of gravity are plotted versus range distance z for a large spin stabilized projectile.

2. Figures A31 and A32 are plots of  $\delta_V$  versus  $\delta_H$  for a spin stabilized and a fin stabilized missile, respectively. Seen here are the expected epicycle plots.

3. Figure A34 is a typical plot of the graphical first approximation to the yawing equation in which the five yaw vectors have been rotated by a chosen slow rate  $\phi_2^1$ .

4. Figure A35 is a plot of the zero-yaw drag force coefficient  $K_D$  versus Mach number for a spin stabilized projectile.

5. Figure A36 is a plot of  $\delta_V^2 + \delta_H^2$  versus range length  $z$ . This plot graphically demonstrates the period of the yawing motion and the fact that the amplitude is damping.

6. Figure A37 is a plot of  $K_M$ , the overturning moment coefficient and  $K_N$ , the normal force coefficients versus Mach number for a spin stabilized projectile.

7. Figure A38 is a plot of  $K_T$ , the Magnus moment coefficient and  $K_H - K_{MA}$ , the damping moment coefficient, versus Mach number.

## 8. REPRESENTATIVE PROGRAMS

Models or full scale projectile up to eight inches in diameter or wing span can be tested in the Transonic Free Flight Range. In the eight years of its operation, much experience has been accumulated in the launching, instrumentation, and data reduction techniques for models of bombs, guided missiles and aircraft; as well as for the more conventional ballistic shapes. Valuable data have been obtained from the successful testing of live (self-propelled) rockets. Models have been launched backward, sideward, and at various lesser initial angles of attack. Two-stage models, with separating sections, have been successfully tested. It may be said that anything with reasonable dispersion can be studied in free flight at this facility.

The spread of Mach numbers covered by range programs has been from 0.2 through 6. Within the very near future, however, the range will have a light-gas gun capable of propelling models up to Mach number 11.

In addition, instrumentation is under study for telemetering from models in flight, such data as heat transfer and base pressure.

## 9. SUMMARY

The Transonic Free Flight Range, a facility which has been in full operation since 1950, is capable of testing missiles up to eight inches in diameter or wing span over a Mach number range of 0.2 to 6. It is capable of supplying data that gives a complete history, over 700 feet of its trajectory, of the motion of the missile. From this data can be derived the aerodynamic properties and the flow phenomena associated with the missile in free flight.

High-speed motion picture cameras and other techniques furnish detailed information about launching parameters. This information, together with that obtained from a 1000-yard target incorporated with the range facilities, makes possible the study of dispersion problems.



WALTER K. ROGERS, JR.

## 10. REFERENCES

1. Rogers, Walter K., Jr. The Transonic Free Flight Range.  
Aberdeen Proving Ground: BRL R-849, Feb 53.
2. Braun, Walter F. The Free Flight Aerodynamics Range.  
Aberdeen Proving Ground: BRL R-1048, May 58.
3. Bennett, F. D. The Controlled-Temperature-Pressure Range.  
Paper presented at Aerodynamics Range Symposium,  
published in proceedings of symposium (See Reference 10),  
1957. Paper also published in the Aeronautical  
Engineering Review, 16: 63-68, Oct 1957.
4. May, Albert, and Williams, T. J. Free Flight Ranges at the  
Naval Ordnance Laboratory. NAVORD R-4063, July 1955.
5. Staff, Aeroballistics Laboratory. Dynamic Aeroballistic  
Evaluation. NOTS 1152, July 1955.
6. Dunn, Eldon L. Center of Gravity Reduction for NOTS  
Aeroballistics Laboratory. NAVORD 3494, July 1955.
7. Seiff, Alvin. A Free Flight Wind Tunnel for Aerodynamic  
Testing of Hypersonic Speeds. NACA R-1222, May 1955.
8. Briggs, Robert O., Kerwin, William J., and Schmidt, Stanley F.  
Instrumentation of the Ames Supersonic Free Flight Wind  
Tunnel. NACA RM A52A18, 1952.
9. Bull, Gerald V. Some Aerodynamic Studies in the Canadian  
Armament Research and Development Establishment  
Aeroballistics Range. Canadian Aeronautical Journal,  
2: No. 5, 154-163, May 1956.
10. Aerodynamics Range Symposium, Proceedings of; January 1957.  
Aberdeen Proving Ground: BRL Report 1005, Part I and  
Part II, March 1957 (Part II - Confidential).
11. Dickinson, Elizabeth R. Physical Measurements of Projectiles.  
Aberdeen Proving Ground: BRL TN-874, Feb 1954.
12. MacAllister, Leonard C. On the Use of Plastic Sabots for Free  
Flight Testing. Aberdeen Proving Ground: BRL M-792,  
May 1954.
13. Murphy, Charles H. Data Reduction for the Free Flight Spark  
Ranges. Aberdeen Proving Ground: BRL R-900, Feb 1956.



14. Bolz, R. E., and Nicolaides, J. D. A Method of Determining Some Aerodynamic Coefficients from Supersonic Free Flight Tests of a Rolling Missile. Jour. Aero. Sci., 17: No. 10 609-621, Oct 1950. Also Published as BRL R-711.
15. Nicolaides, J. D. On the Free Flight Motion of Missiles Having Slight Configurational Asymmetries. Aberdeen Proving Ground: BRL R-858, June 1953.
16. MacAllister, Leonard C. Comments on the Preliminary Reduction of Symmetric and Asymmetric Yawing Motions of Free Flight Range Models. Aberdeen Proving Ground: BRL R-781, May 1954.
17. Warren, J. R., Templin, R. J., and Cheers, B. Aeroballistics Range Measurements of the Performance and Stability of a Supersonic Aircraft. Institute of the Aeronautical Sciences Preprint No. 788, Jan 1958.
18. Murphy, Charles H. Analogue Computer Determination of Certain Aerodynamic Coefficients. Aberdeen Proving Ground: BRL R-807, April 1952.
19. Schmidt, J. A. A Study of the Resonating Yawing Motion of Asymmetric Missiles by Means of Analog Computer Simulation. Aberdeen Proving Ground: BRL R-922, Nov 1954.
20. Murphy, Charles H. The Measurement of Nonlinear Forces and Moments by Means of Free Flight Tests. Aberdeen Proving Ground: BRL R-974, Feb 1956.
21. Murphy, Charles H. Prediction of the Motion of Missiles Acted on by Nonlinear Forces and Moments. Aberdeen Proving Ground: BRL R-995, Oct 1956. (Also published as The Prediction of Nonlinear Pitching and Yawing Motion of Symmetric Missiles, Jour. Aero. Sci., 24: No. 7 473-479, July 1951.)
22. Clauser, Francis. Choking in Free Flight Ranges. Paper given at Free Flight Symposium, Jet Propulsion Laboratory, 1947.
23. Karpov, B. G. Accuracy of Drag Measurements as a Function of Number and Distribution of Timing Stations. Aberdeen Proving Ground: BRL R-658, Nov 1947.
24. Bull, Gerald V. Aeronautical Studies in the Aeroballistics Range. Canadian Armament Research and Development Establishment Report No. 302/57, July 1957.

## APPENDIX

### Design of the Transonic Range

## APPENDIX

### Design of the Transonic Range

In this section, an attempt has been made to enumerate some of the thoughts and plans which were incorporated in the design of the Transonic Range. When this large range was being contemplated in 1944, the smaller Free Flight Aerodynamics Range<sup>2</sup> was already successfully producing data. However, it was desirable to have a range large enough to allow the study of the properties of full scale service projectiles in free flight.

In order to use the methods and theories available to obtain desired aerodynamic parameters this new large range had to produce certain records. These were:

1. A time-distance history which could give drag.
2. A record of the space coordinates of the center of gravity which would give lift.
3. A record in two known planes of the inclination of the axis of the missile. The period of the oscillations so recorded would give moment data and the amplitudes would give damping data.
4. A record, throughout the range, of the flow characteristics to allow aerodynamic study of flow phenomena through the velocity range encountered. From experience, this requirement, though not imperative, was considered very desirable.

An enclosed range was considered most efficient for the following reasons:

1. To obtain the accuracy in final aerodynamic coefficients and to obtain those coefficients through the solution of the equations of motion using existing theories, it was considered desirable to have a high density of observations in the initial stages of flight where the yawing motion is usually most pronounced.
2. The instrumentation should be protected from the elements and the range survey must have a high degree of accuracy.
3. The practical consideration of greater ease of control for photographic techniques necessitated a light tight enclosure.
4. The air should be still and practically constant in its properties.



The design of the enclosed range building was planned in the following manner. Since it was desired to obtain useful information about a missile's aerodynamic properties within the transonic velocity range, the problem of choking was considered. At that time, little was known of this property with the exception that wind tunnels were universally unreliable within certain limits near the speed of sound. Dr. Theodore Von Karman, Chairman of Advisory Group for Aeronautical Research and Development, NATO, suggested that a ratio of 10,000/1, cross section of range to projectile, should be sufficient to practically eliminate this effect in the range. Using a 3-inch diameter shell as a basis, this meant that the unobstructed range cross section should be at least 22 x 22 feet. Dr. Francis Clauser, a member of the Scientific Advisory Committee for the Ballistic Research Laboratories, has since proved that ranges will choke in much the same fashion as wind tunnels<sup>22</sup>. If it is desired to test projectiles at very low velocities then it must be considered that the velocity attainable is dependent on the range cross section and length, the position of the launching device and the allowable proximity of projectile to instrumentation. Furthermore, with high arcing trajectories the photographic techniques are complicated.

To obtain a large number of experimental observations, a long range was desirable. It is known<sup>23</sup> that the drag error varies inversely with the square of range length if absolute accuracy of length and time are invariant. Also, the accuracy of length measurement varies only with the first power of total distance. A long range, however, again would restrict the low range of velocities if impacts within the range were considered impractical. Furthermore, dispersion was estimated to vary between the first and second power of the range length. In the smaller Aerodynamics Range the dispersion was found to be normally about 1-1/2 feet at 300 feet from the launcher. Using a possible figure of 700 feet for the large range length this rule would indicate a dispersion of about 6 feet. This figure for dispersion has proved to

be approximately correct. The range length was designed to be 750 feet. Financial considerations, however, played a considerable part in this limit. The range is now 1173 feet long. The last extension of 423 feet is, as yet, uninstrumented except with yaw cards.

The design of the apparatus for obtaining data leaned heavily on the experience gained in the smaller, but already successfully proven, Free Flight Aerodynamics Range<sup>2</sup>.

The difference in requirements for the two ranges was obvious. The projectiles to be fired in this large range could be 8 inches in diameter and 5 feet in length while the maximum size for the smaller range was about 2 inches in diameter and 10 inches in length. The size of the field of view required in this larger range was much greater. As discussed above, the size of clear flight space to satisfy choking requirements, trajectory, and dispersion was to be about 22 feet x 22 feet.

This difference suggested that direct photography might be used instead of spark, shadow photography. However, the depth of field required by a six foot dispersion and the location of the projectile in space made this impractical. The latter, though not too complicated, would be expensive, requiring each camera to be precision made and mounted and a system of fiducial marks to be placed within the camera and surveyed as such. Also, experience indicated there was value to be obtained from the shadow photographs in which the compressible flow phenomena could be studied throughout the flight within the range.

Therefore, the use of spark photography in this large range was studied. The desired flow characteristics would be obtained and the dispersion and depth of field problems would be lessened. With direct shadow photography, however, the records would be 12 feet square and, due to the large distance involved, an increase in light, over that

obtained from the spark source then in use in the Aerodynamics Range, would be necessary. The larger records were impractical but the motion picture analogy solved the problem. A reflective screen was placed at the side and top of the range and an ordinary still camera used in place of the eye of the audience. This technique solved one problem but the second was intensified, since now the light requirement increased. To obtain more light it was necessary to employ higher voltage and capacity. While the Aerodynamics Range used 6 KV at  $.5\mu\text{F}$ , the larger range was to use 15 KV at  $.25\mu\text{F}$ . This was accomplished by the use of a confined air gap spark of the Libessart type. A picture of this gap is presented in Figure A5. The light was now bright enough to expose a very fast spectroscopic plate to good density; the duration, however, was about 3 microseconds, giving a distance error of about  $1/16$  inch at a projectile velocity of 2,000 ft/sec.

The Transonic Range building was thus designed and completed and the basic instrumentation contracted for in 1947 and has, at present, been in successful full-scale operation for about eight years.

## 12. FIGURES

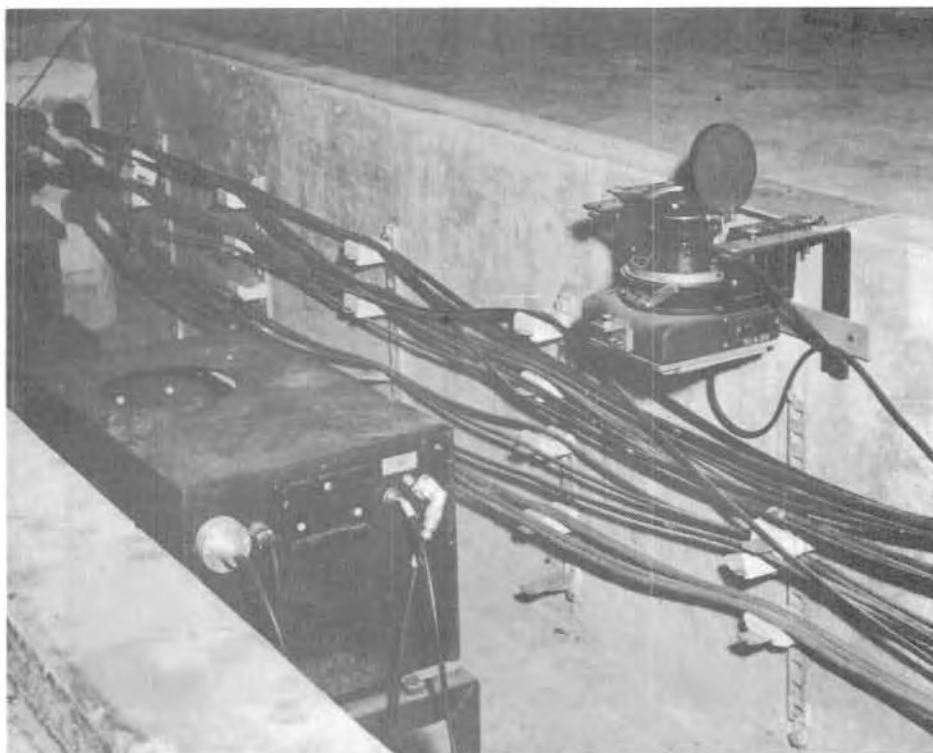


Fig. A4 View of Spark Box (Light Source)  
and Camera Set-up.

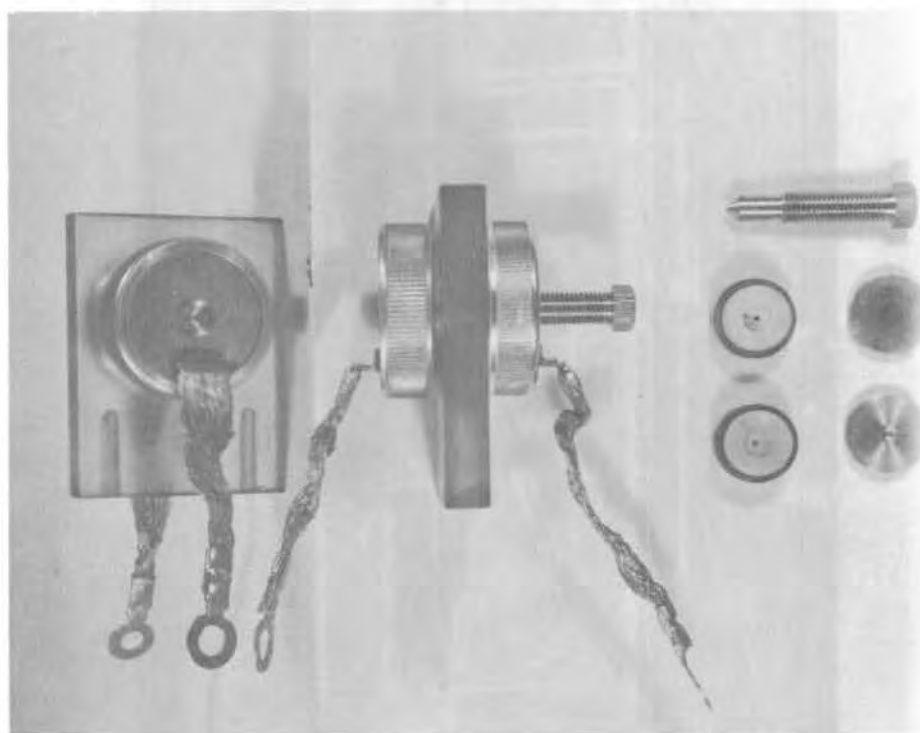


Fig. A5 - Confined Air Gap Spark  
(Libessart Type)

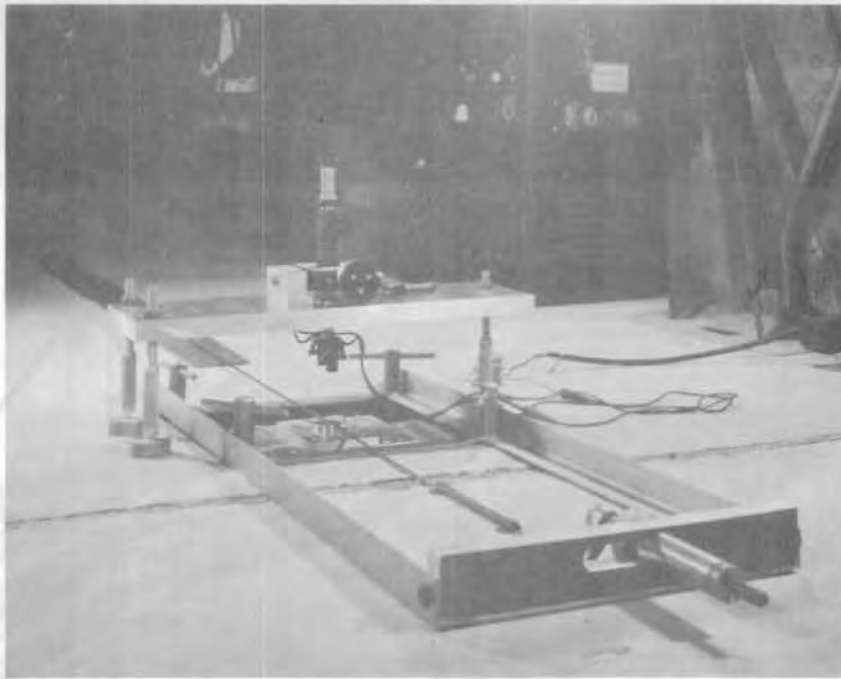


Fig. A6 - Range Survey Set-Up  
Showing Taping Operation over primary bench marks

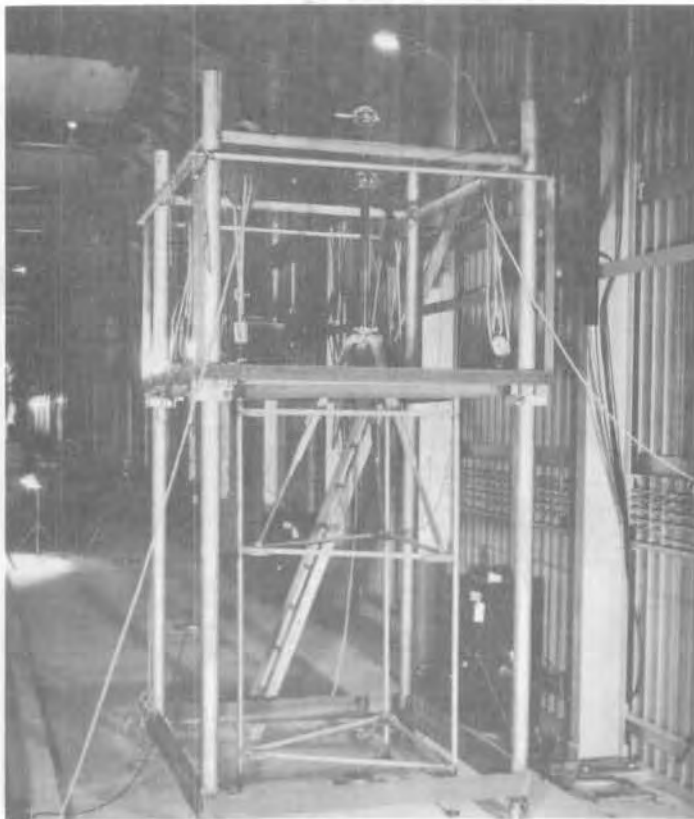


Fig A7 - Range Survey Set-Up  
Showing mobile stand for theodolite positioned over  
primary bench mark.

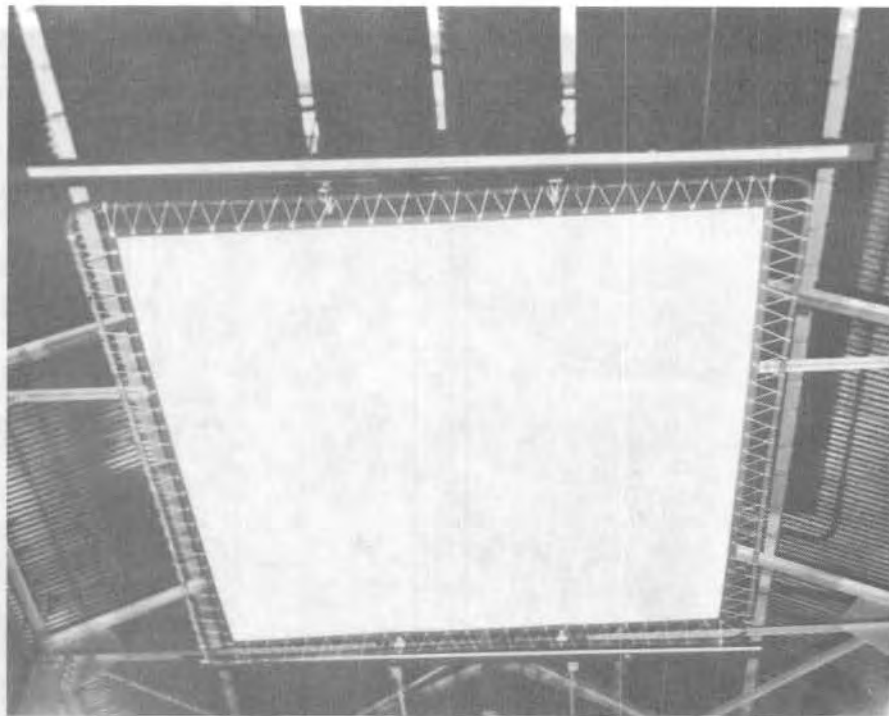


Fig. A8 - Reflective Strip for Photocell Light Trigger  
(Just preceding each large reflective screen)

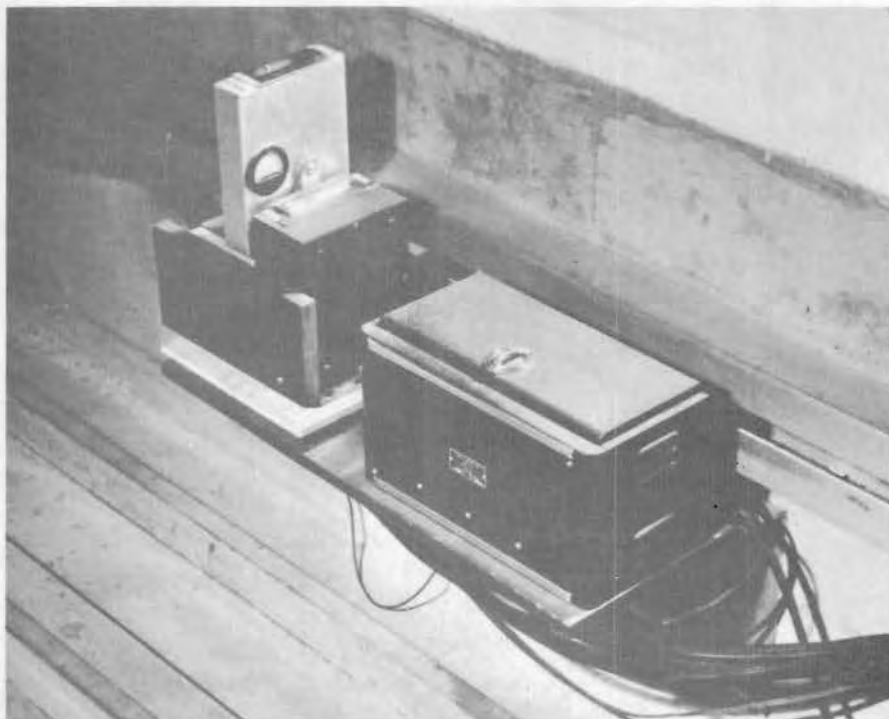


Fig. A9 - Photocell Unit. Note Two cylindrical  
lenses for collimation of light sheet.



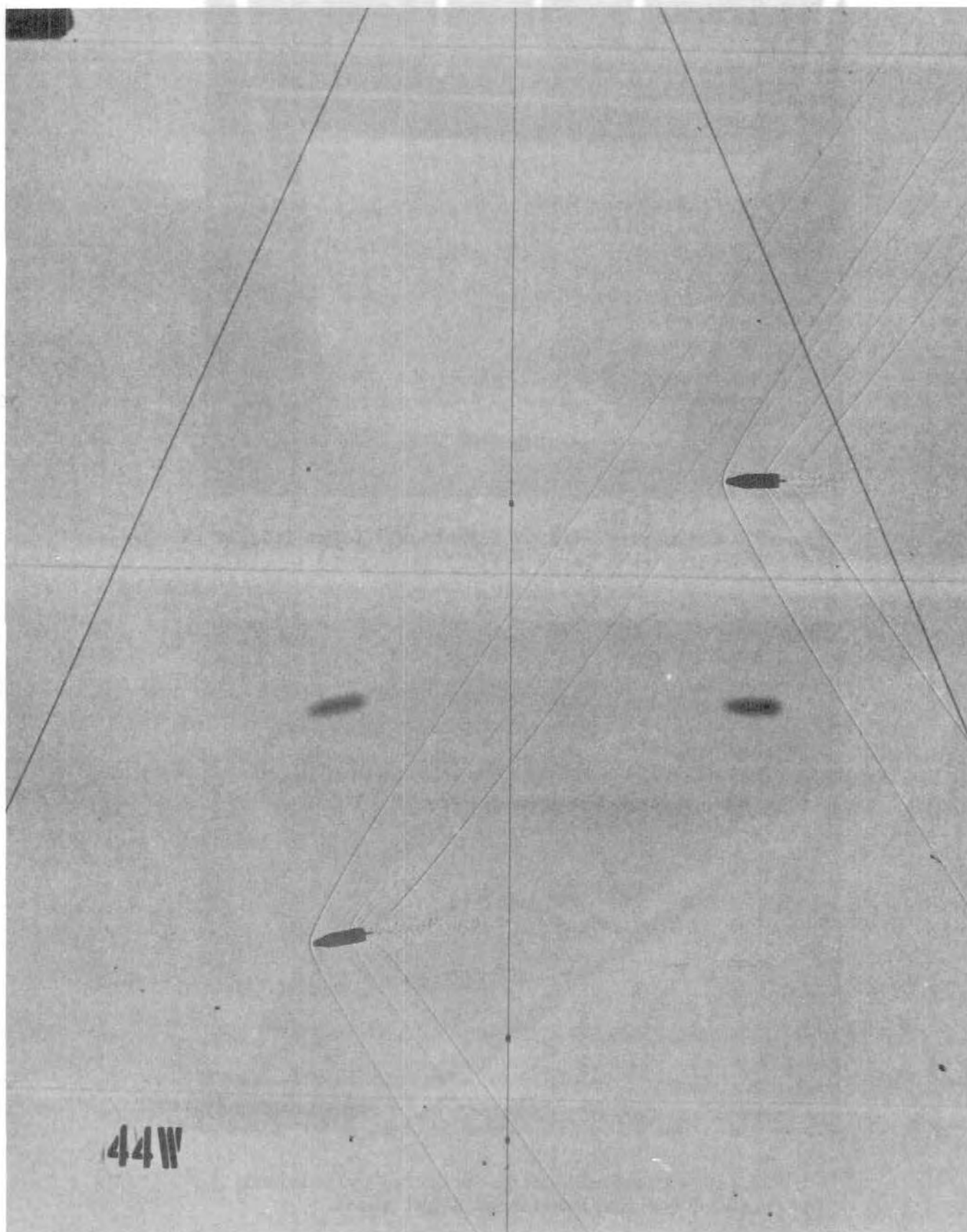


Fig. A10 - Example of dual shadowgraph obtained by discharge of two sparks with short interval of time between them. 20mm projectile.



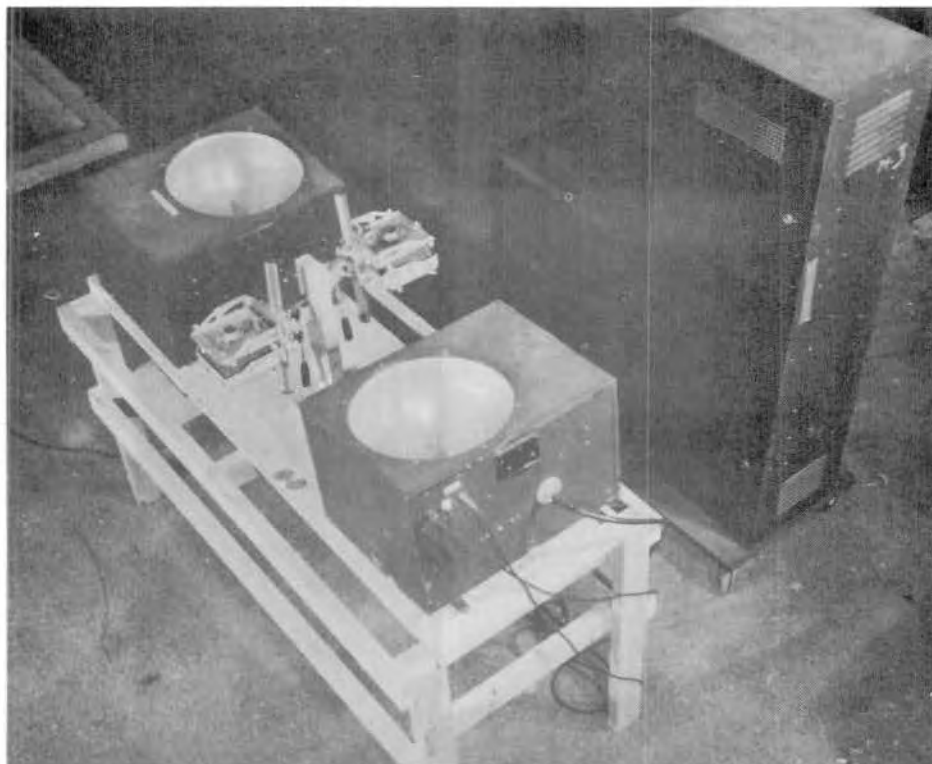


Fig. A11 - Microflash (Direct Photography) Set-Up.  
Showing double camera and light source

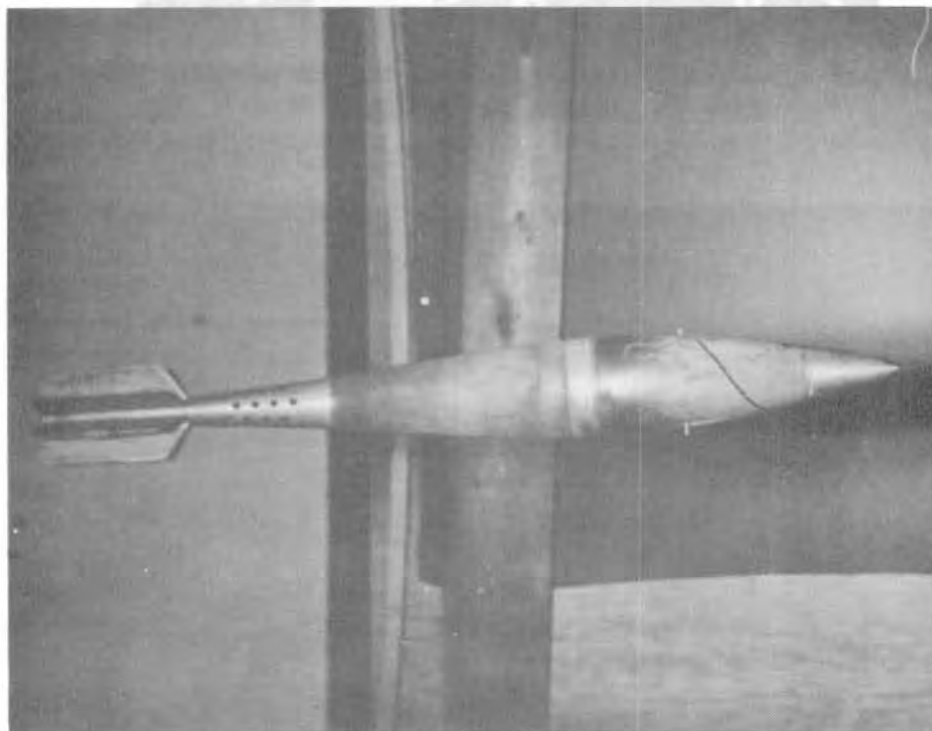


Fig. A12 - Microflash (Direct Photograph).  
Velocity: Approx. 985 ft./sec.  
Mach No.: Approx. .88



Fig. A13 - Mosaic (Multiple Plate) Set Up. Showing Small Spark in Ceiling Above Plate Table

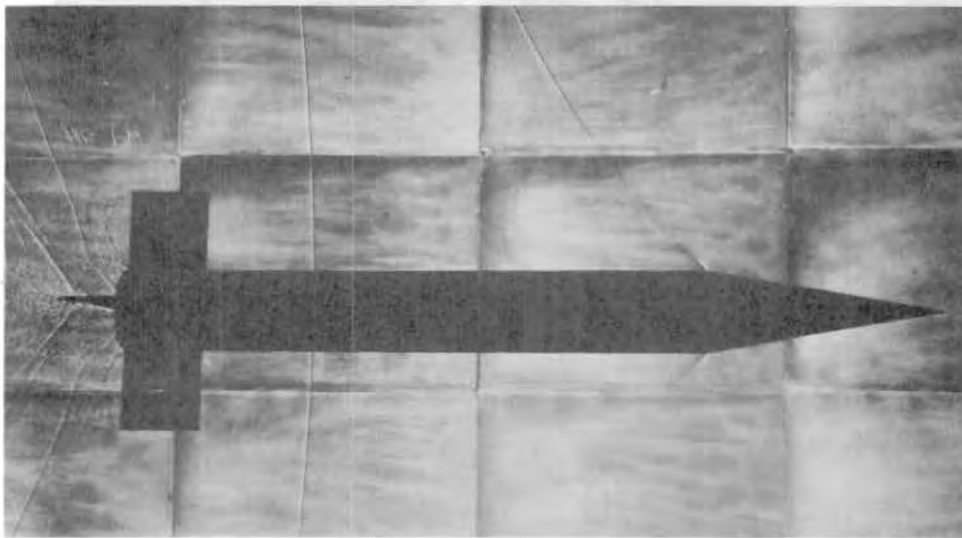


Fig. A14 - Large Mosaic (Multiple Plate). Shadowgraph of Finned Cone Cylinder  
Velocity: Approx. 1170 ft/sec  
Mach No.: Approx. 1.04



Fig. A16 - Exterior of Instrument Shelter



Fig. A17 - Interior View of Instrument Shelter  
Showing control console and electronic counters.



Fig. A18 - Exterior View of Temperature Controlled Magazine and Loading Facility

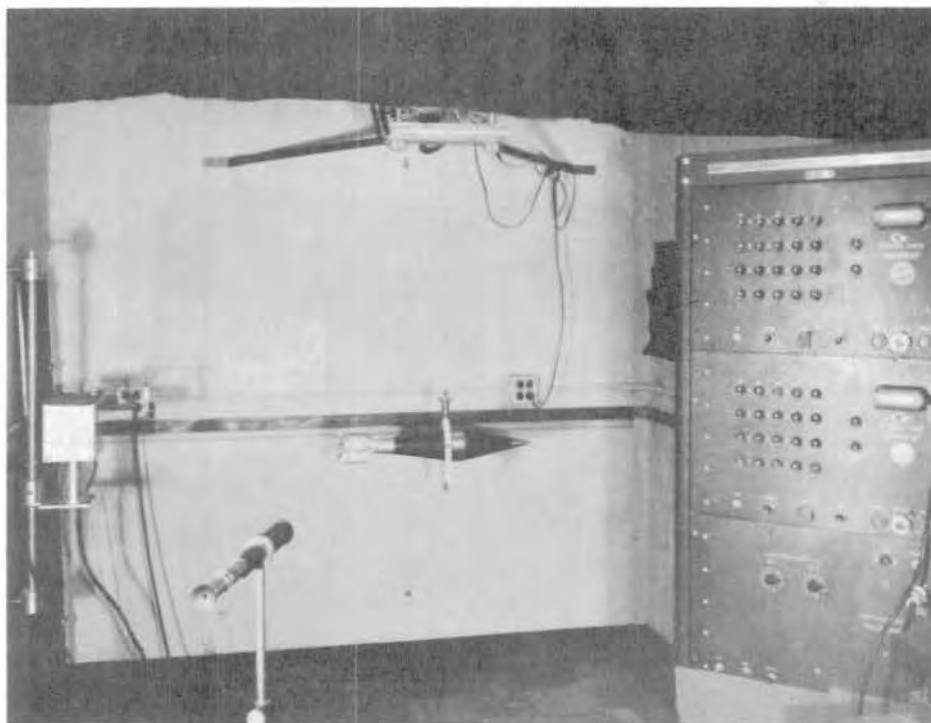


Fig. A19 - Torsion Pendulum  
Physical Measurements Section  
(105 mm Shell Suspended)

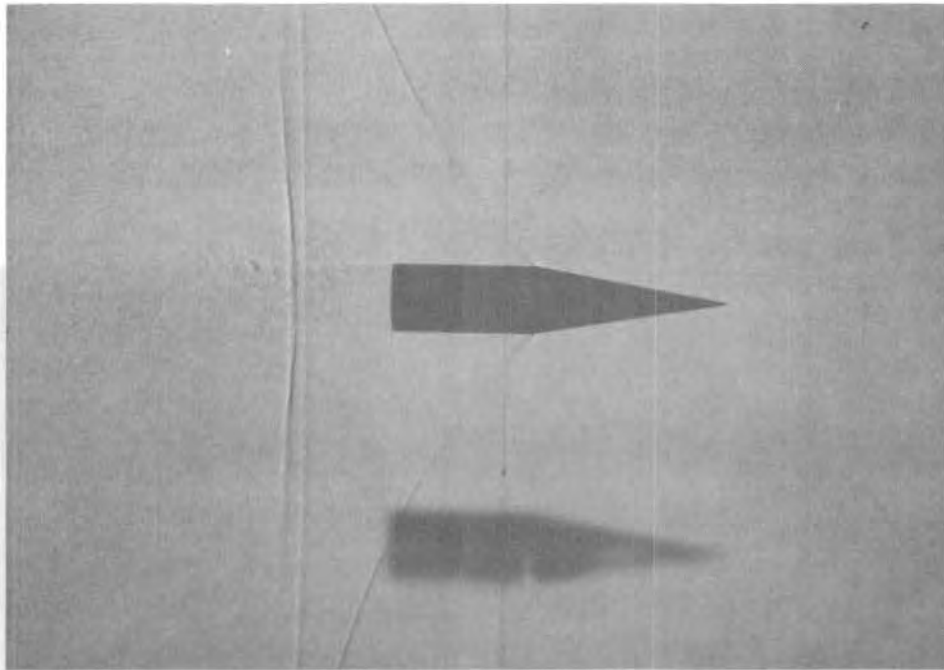


Fig. A21 - Shadowgraph of 90mm Cone Cylinder  
Velocity: Approx. 1128 ft/sec  
Mach No.: Approx. 1.0

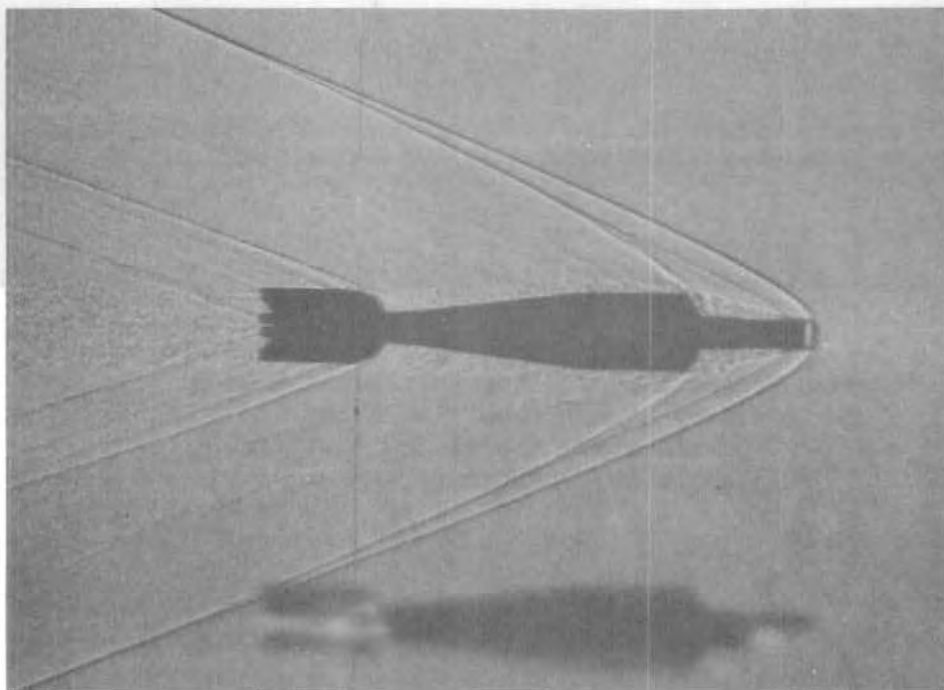


Fig. A22 - Shadowgraph of 90mm Finned Projectile  
Velocity: Approx. 3350 ft/sec  
Mach No.: Approx. 2.95

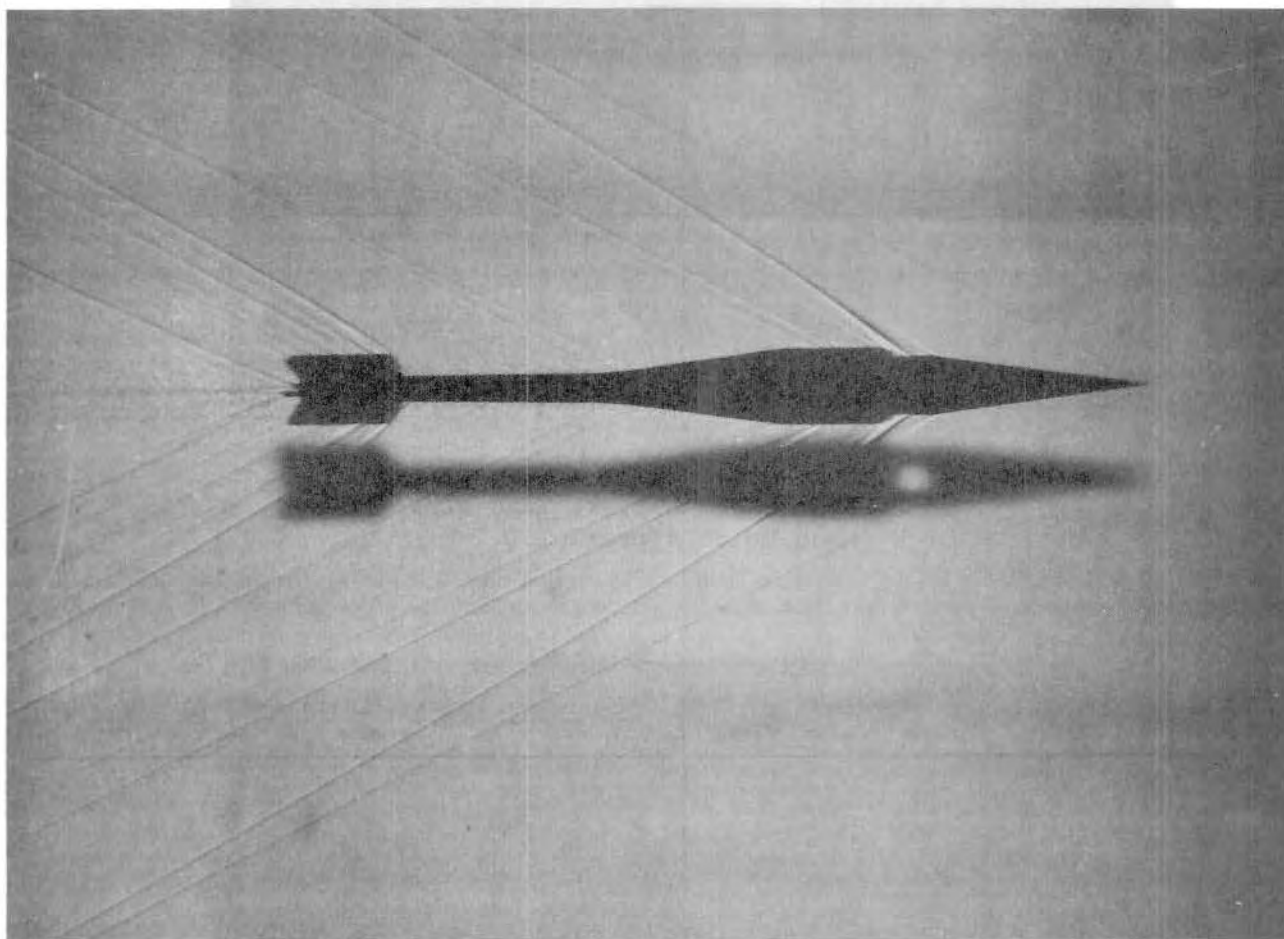


Fig. A23 - Shadowgraph  
 90mm Projectile with Special Research Cone  
 for Boundary Layer Transition Study.  
 Velocity: Approx. 2414 ft/sec  
 Mach No.: Approx. 2.15



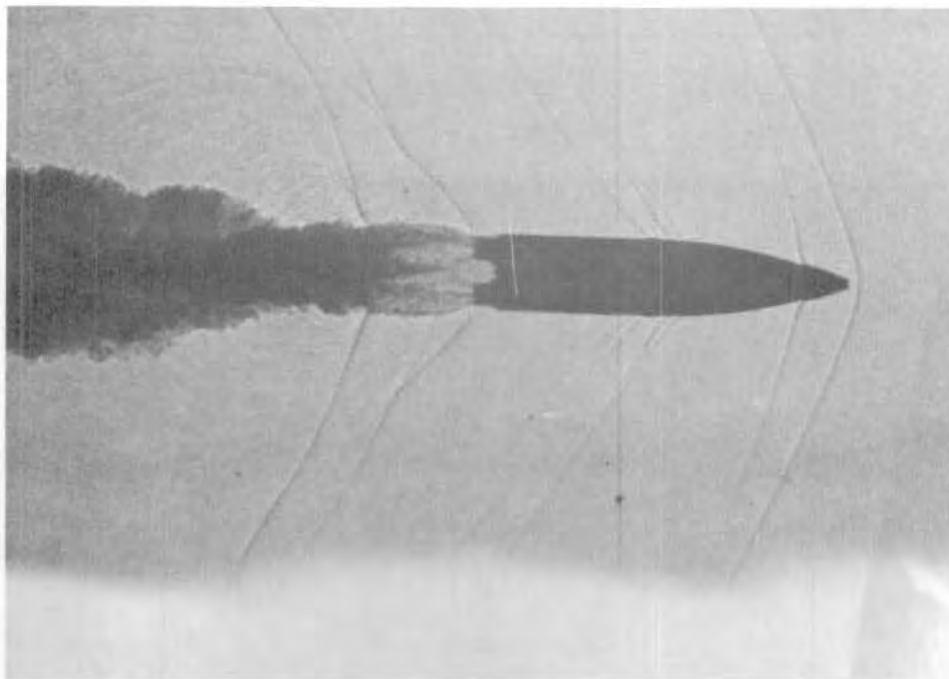


Fig. A24 - Shadowgraph of Burning Rocket  
Velocity: Approx. 1200 ft/sec  
Mach No.: Approx. 1.06

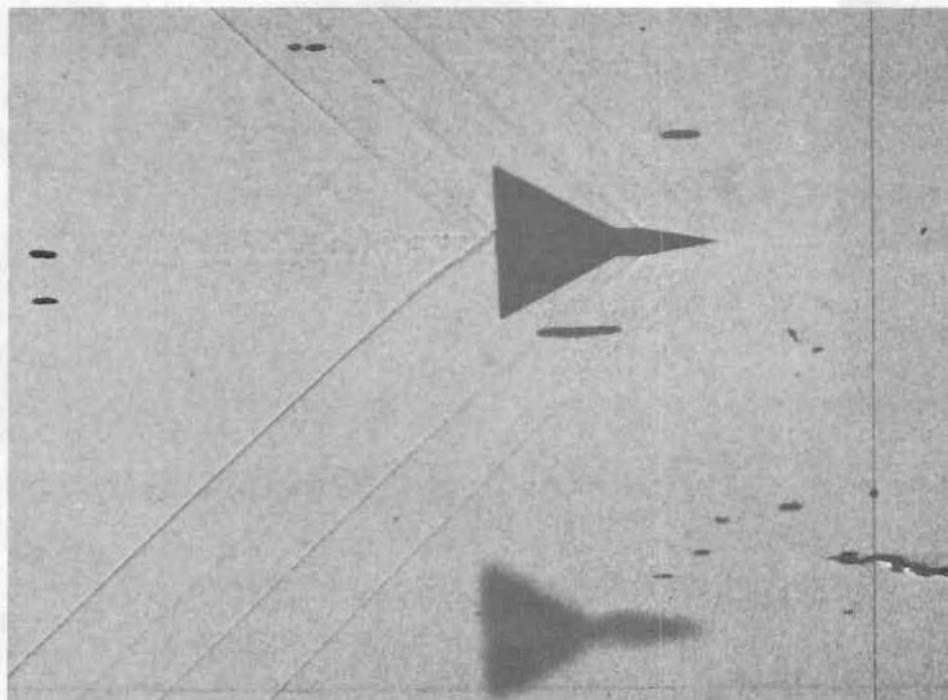


Fig. A25 - Shadowgraph of Delta Wing  
Aircraft Model  
Velocity: Approx. 1570  
Mach No.: Approx. 1.4

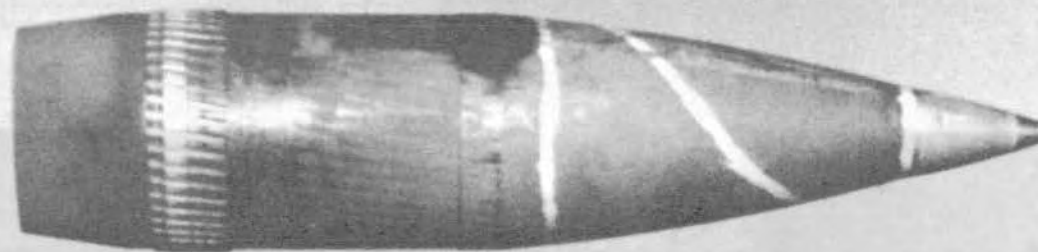


Fig. A26 - Direct or Microflash Photograph  
of 155mm Projectile  
Velocity: Approx. 630 ft/sec  
Mach No.: Approx. .55

Fig. A27 - Enlarged Print From 16mm Fastax Motion picture film showing finned projectile and separation of plastic sabot fragments.

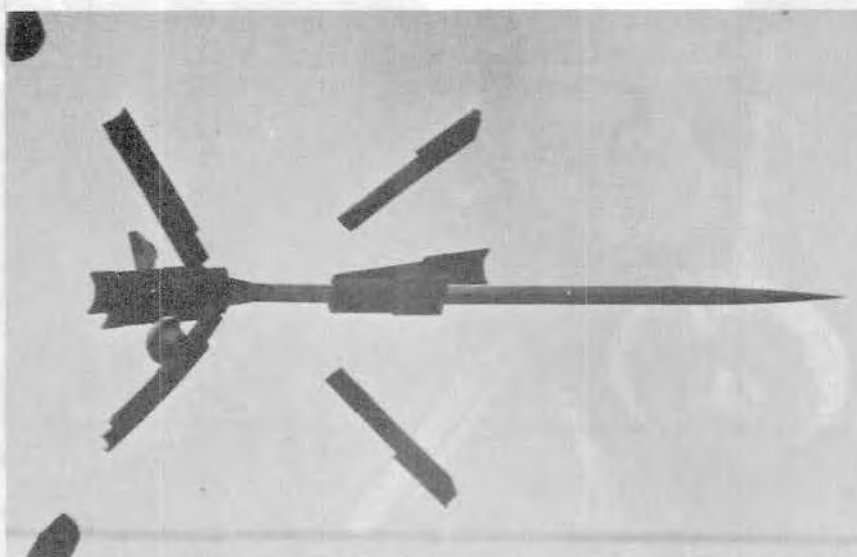
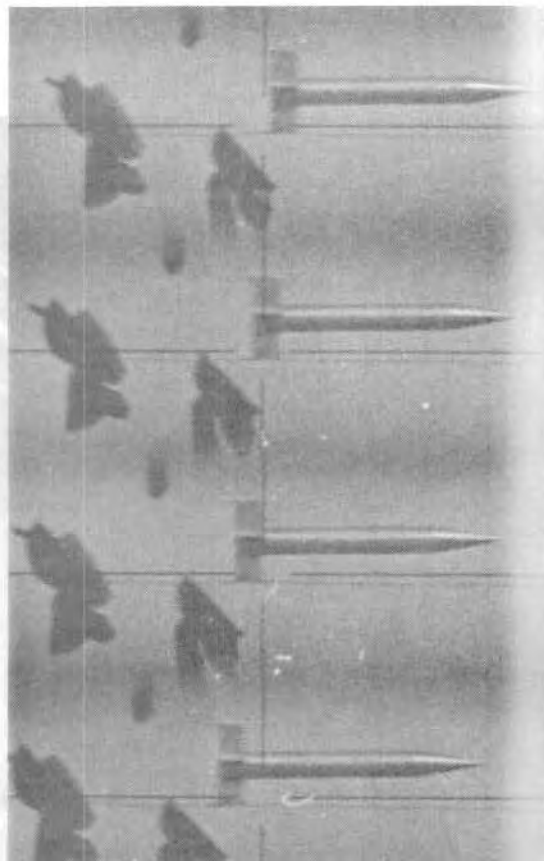


Fig. A28 - Enlarged Print From Fastax Motion picture film using "Smear" technique. Projectile may be seen emerging from plastic sabot.

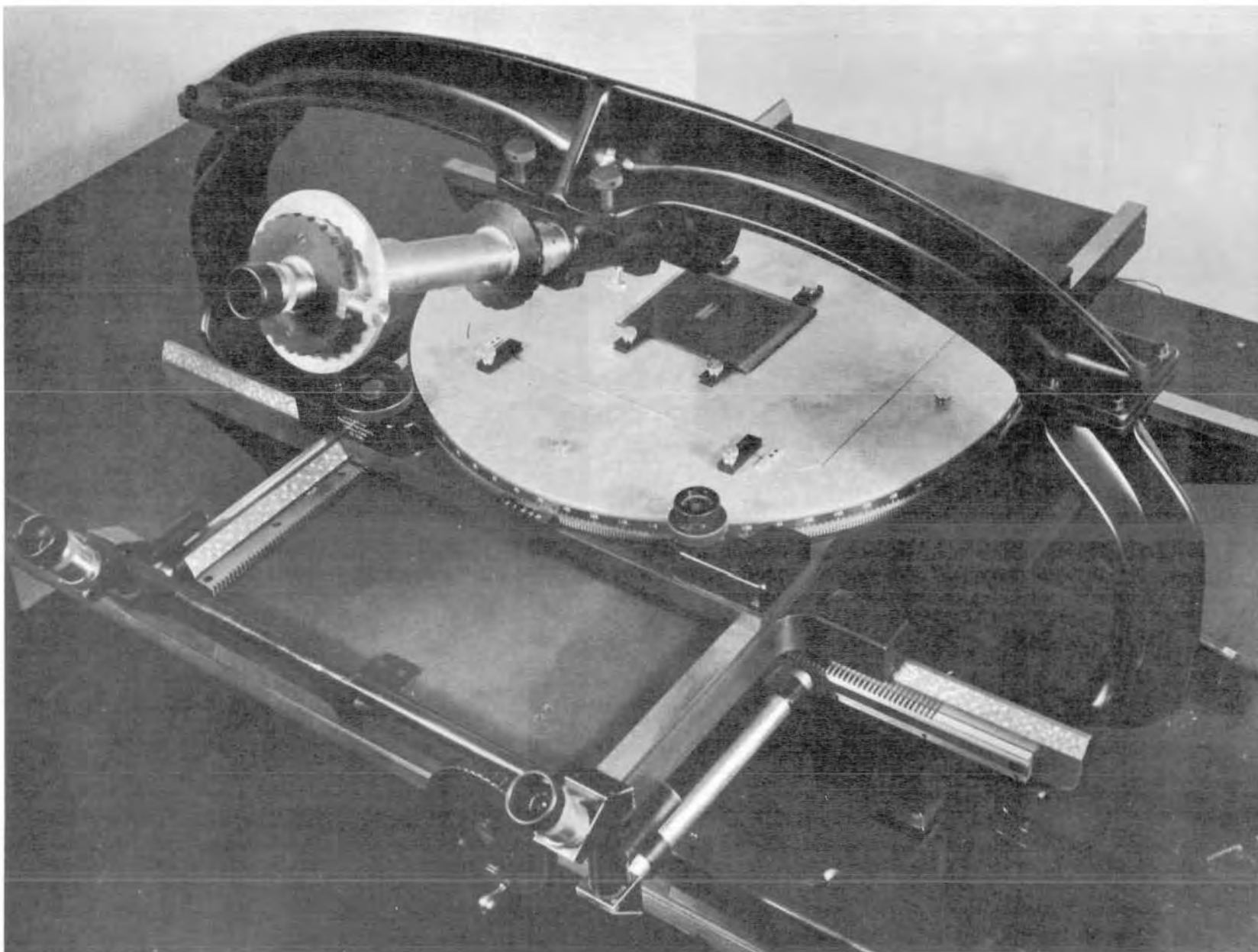


Fig. A29 - Optical Comparitor,  
Reduction Section

FIG. A30

TYPICAL PLOT  
X & Y vs Z

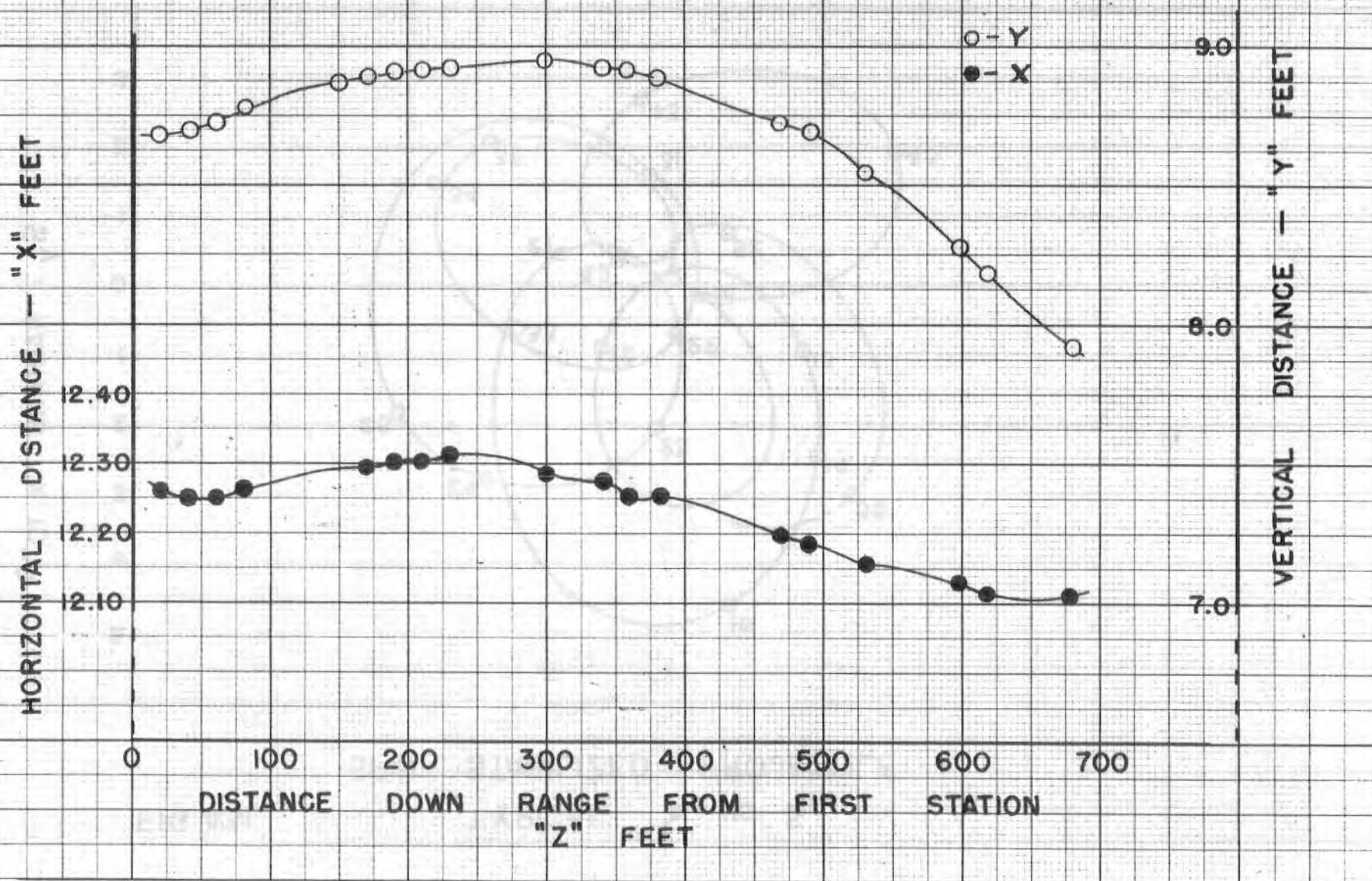




FIG. A31

TYPICAL  $\delta_V$  vs  $\delta_H$   
SPIN STABILIZED PROJECTILE

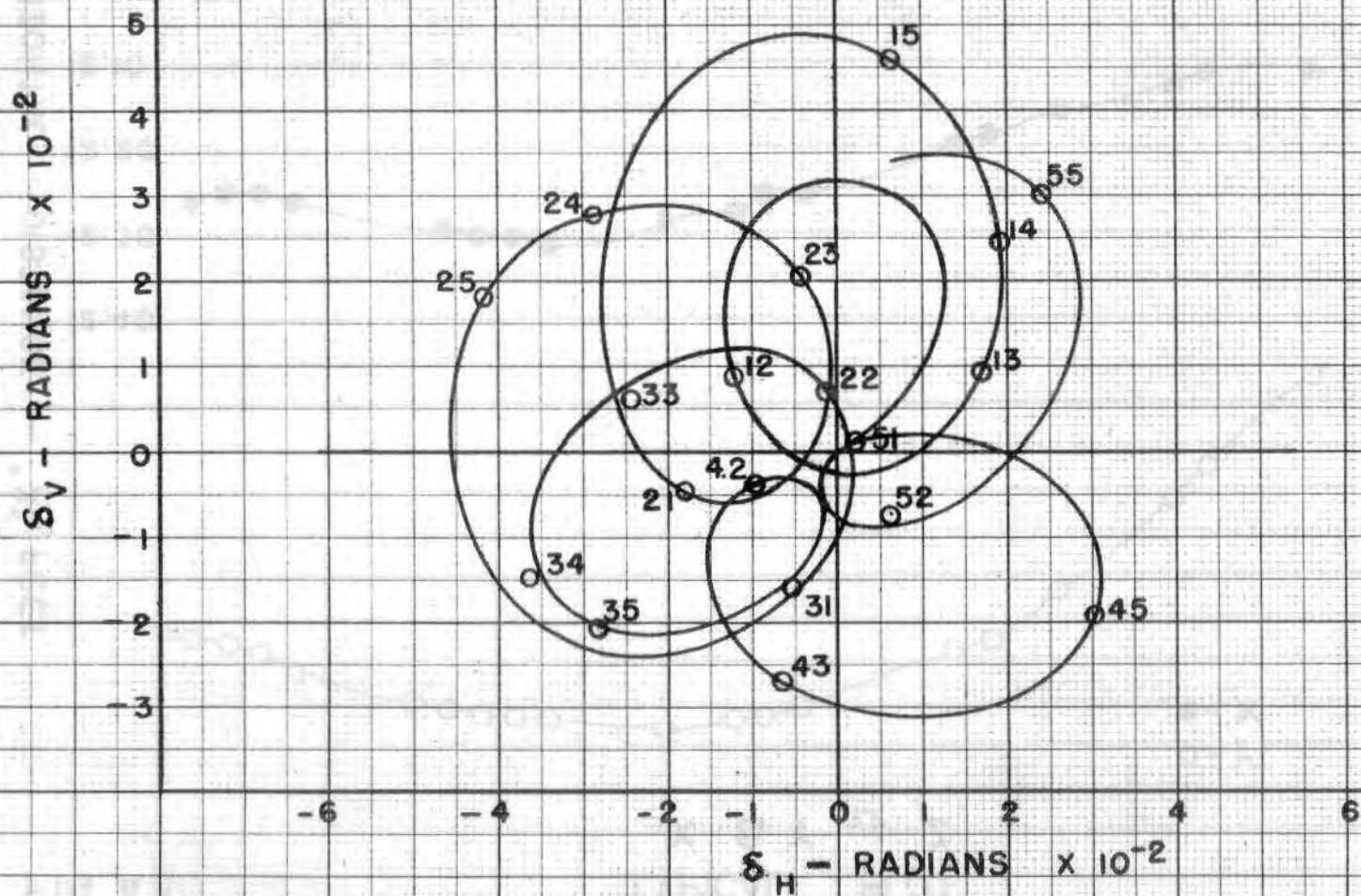




FIG. A32

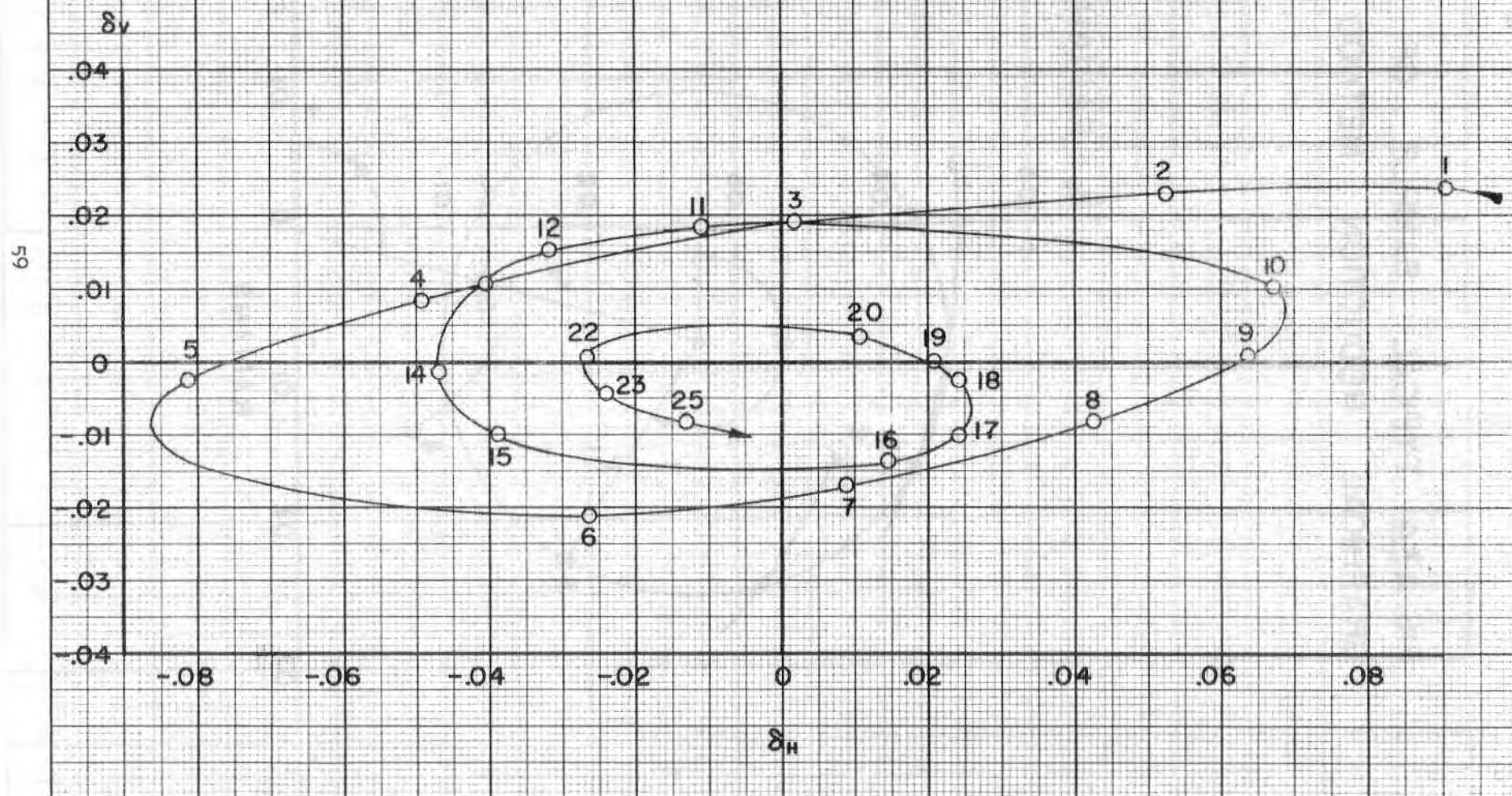
TYPICAL  $\delta_v$  vs  $\delta_H$   
FOR FIN STABILIZED PROJECTILE

FIG. A34 TYPICAL SAMPLE OF  
GRAPHICAL REDUCTION METHOD

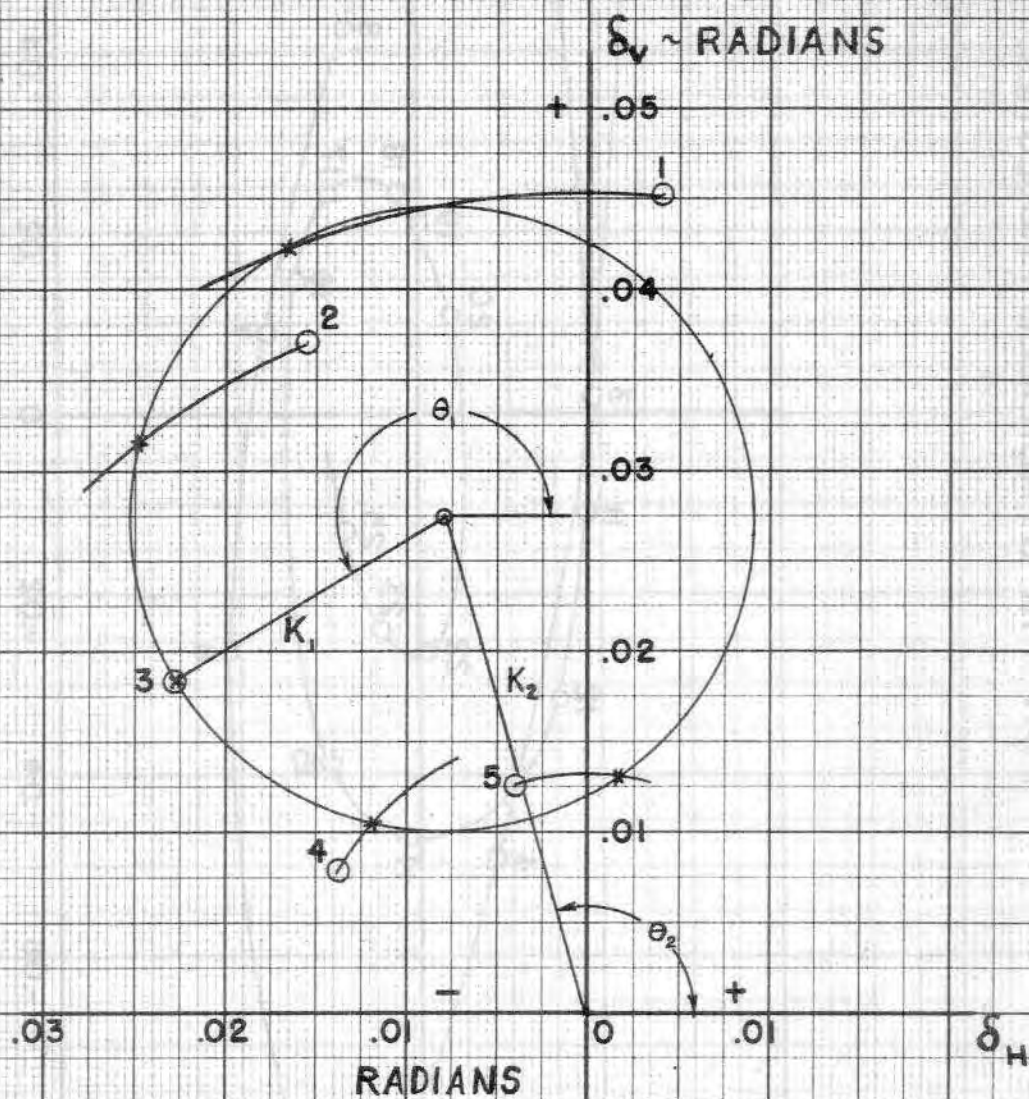


FIG. A35

ZERO-YAW DRAG FORCE COEFFICIENT  
VS  
MACH NUMBER





FIG. A36

TYPICAL PLOT

$$\delta_H^2 + \delta_V^2 \text{ vs } Z$$

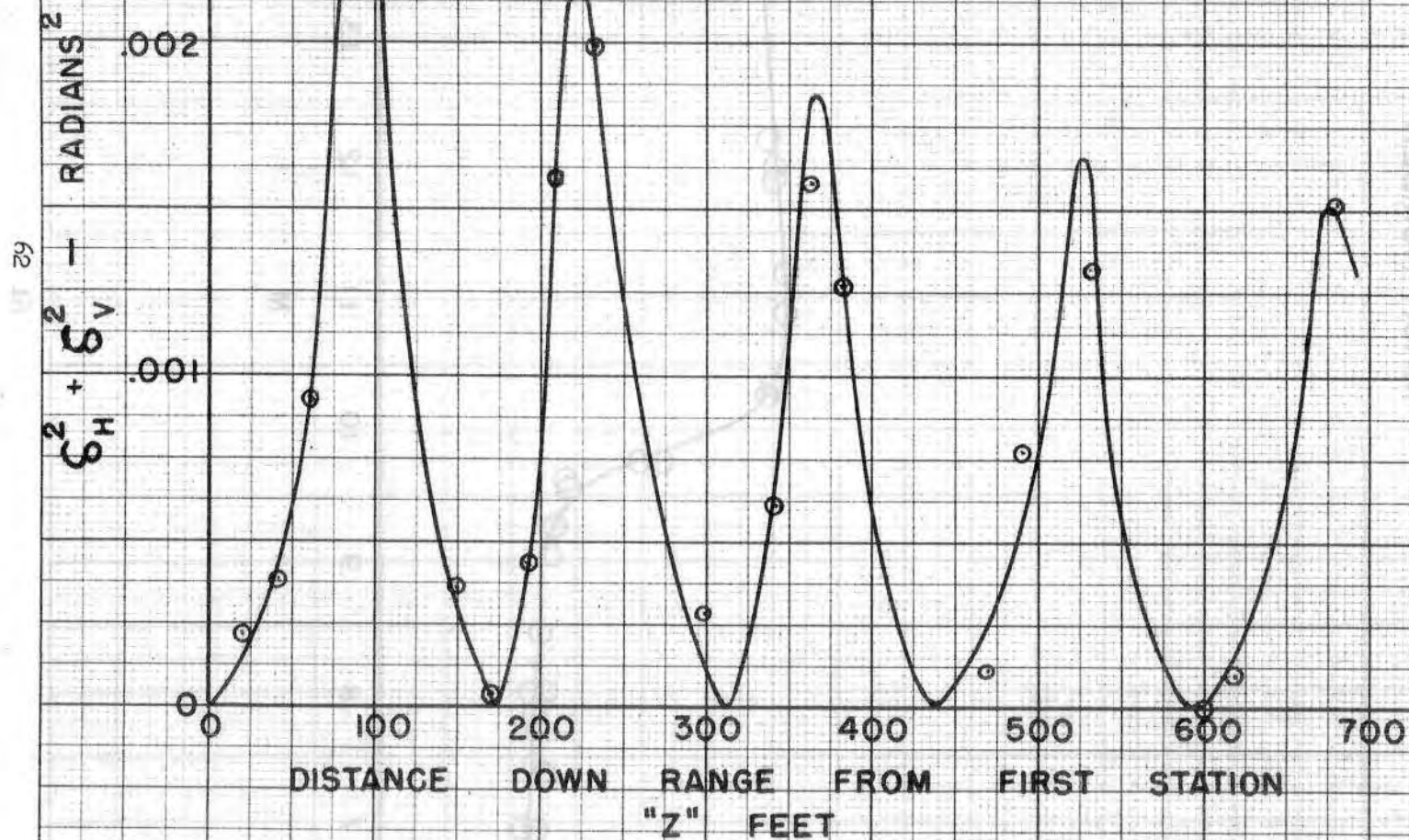


FIG.A37

# OVERTURNING MOMENT COEFFICIENT VS MACH NUMBER

$K_M$

2.4

2.0

1.6

## NORMAL FORCE COEFFICIENT VS MACH NUMBER

$K_N$

0.8

0.6

0.4

● Two C.G.  
○ Swerve

7

8

9

10

11

12

13

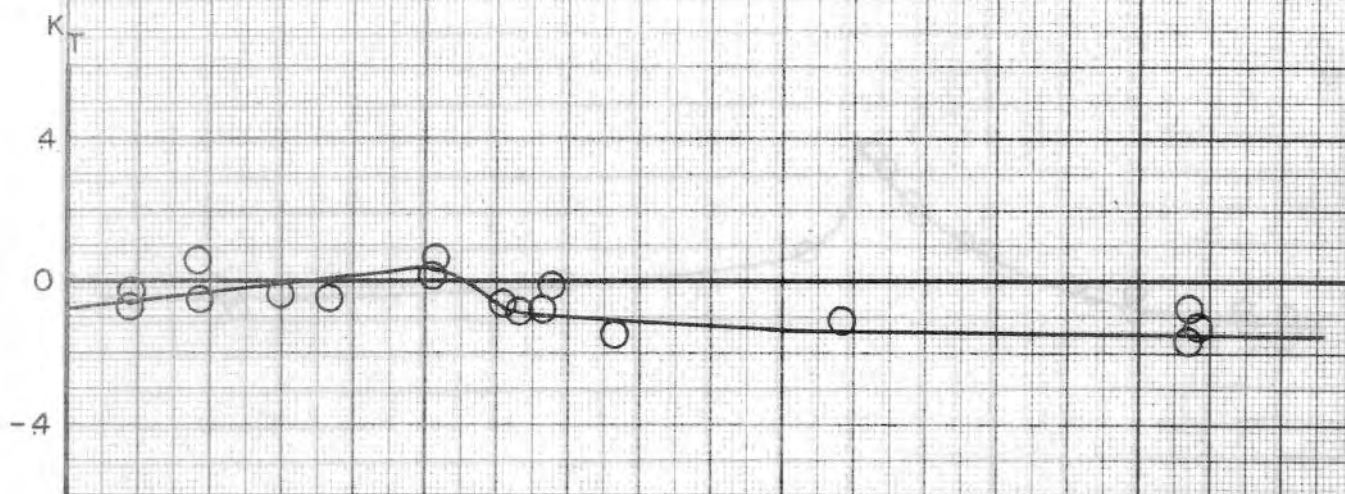
14

15

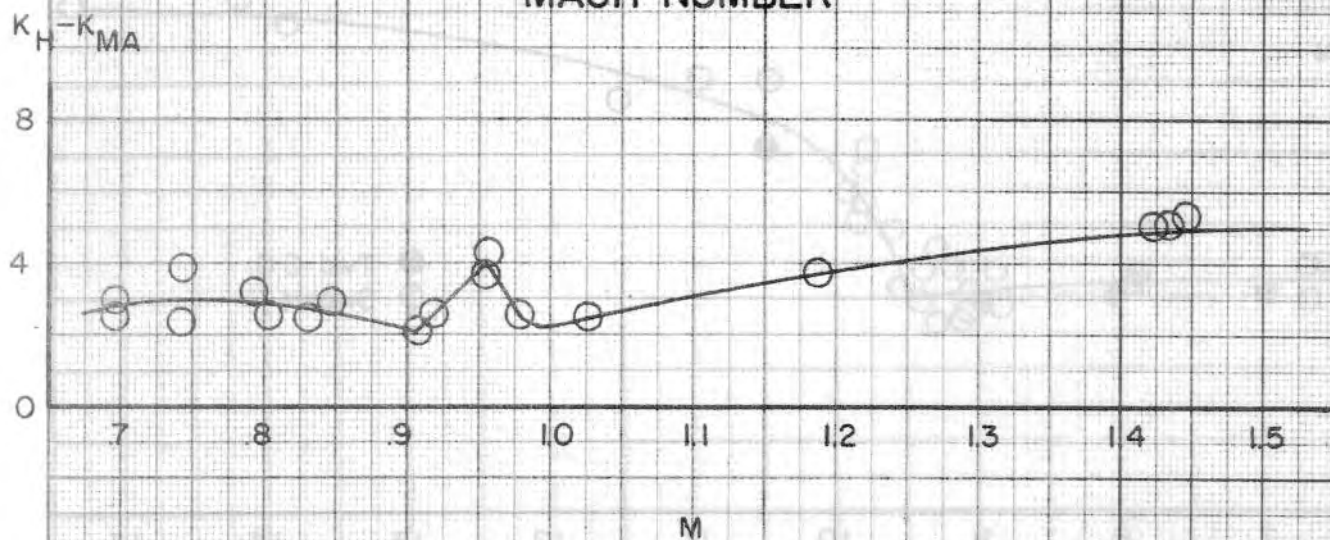
M

FIG. A38

# MAGNUS MOMENT COEFFICIENT VS MACH NUMBER



# DAMPING MOMENT COEFFICIENT VS MACH NUMBER





# DISTRIBUTION LIST

<u>No. of Copies</u>	<u>Organization</u>	<u>No. of Copies</u>	<u>Organization</u>
1	Chief of Ordnance Department of the Army Washington 25, D. C. Attn: ORDTB - Bal Sec	2	Commander Naval Ordnance Laboratory White Oak Silver Spring, Maryland Attn: Dr. Kurzweg Dr. May Mr. Nestinger
10	British Joint Services Mission 1800 K Street, N. W. Washington 6, D. C. Attn: Mr. John Izzard, Reports Officer	5	Commander Naval Ordnance Test Station China Lake California Attn: Technical Library
	Of Interest to: Dr. Simmons - Ministry of Supply Armament Division Kent, England	1	Superintendent Naval Postgraduate School Monterey, California
7	Canadian Army Staff 2450 Massachusetts Ave. Washington 8, D. C.	1	Commanding Officer Naval Aviation Ordnance Test Station Chincoteague, Virginia
	Of Interest to: Adalia Limited Montreal, P. Q. Canada	1	Commander Naval Air Missile Test Center Point Mugu, California
	CANADAIR Montreal, P. Q. Canada	1	Commander Naval Air Development Center Johnsville, Pennsylvania
	Canadian Westinghouse Company Hamilton Ontario, Canada	1	Commanding Officer Naval Air Rocket Test Station Lake Denmark Dover, New Jersey
3	Chief, Bureau of Ordnance Department of the Navy Washington 25, D. C. Attn: ReO	1	Commanding Officer and Director David W. Taylor Model Basin Washington 7, D. C. Attn: Aerodynamics Lab.
1	Commander Naval Proving Ground Dahlgren, Virginia		

# DISTRIBUTION LIST

<u>No. of Copies</u>	<u>Organization</u>	<u>No. of Copies</u>	<u>Organization</u>
2	Commander Wright Air Development Center Wright-Patterson Air Force Base, Ohio Attn: WCLG	1	Director National Advisory Committee for Aeronautics Langley Memorial Aero- nautical Laboratory Langley Field, Virginia
1	Commander Air University Maxwell Air Force Base, Alabama Attn: Library	1	Director National Advisory Committee for Aeronautics Lewis Flight Propulsion Laboratory Cleveland Airport Cleveland, Ohio
1	Chief of Staff U. S. Air Force The Pentagon Washington 25, D. C. Attn: DCS/D, AFDRD-AC-3	10	Director Armed Forces Technical Information Agency Arlington Hall Station Arlington 12, Virginia Attn: TIPDR
1	Commander Air Research and Development Command Andrews Air Force Base Washington 25, D. C.	1	Chief of Staff, US Army Research & Development Washington 25, D. C. Attn: Director/Research
1	Commander Ballistic Missiles Division Air Research and Development Command P. O. Box 262 Inglewood, California Attn: WDSIT WDTLA	2	Office Asst. Sec. of Defense (R&E) Washington 25, D. C. Attn: Director/Ordnance Director/Guided Missiles
2	Director National Advisory Committee for Aeronautics Ames Aeronautical Laboratory Moffett Field, California Of Interest to: Dr. A. C. Charters	2	Commanding General Frankford Arsenal Philadelphia 37, Pa.
1	Director National Advisory Committee for Aeronautics 1512 H Street Washington 25, D. C.	1	Commander Arnold Engineering Develop. Center Tullahoma, Tennessee Attn: Deputy Chief, Staff R and D

# DISTRIBUTION LIST

<u>No. of Copies</u>	<u>Organization</u>	<u>No. of Copies</u>	<u>Organization</u>
1	U. S. Atomic Energy Commission Sandia Corporation P. O. Box 5900 Albuquerque, New Mexico	1	Commanding Officer Diamond Ordnance Fuze Laboratories Washington 25, D. C. Attn: ORDTL - 06,33
1	Development Division Field Command, AFSWP Sandia Base Albuquerque, New Mexico	1	Commanding Officer Watertown Arsenal Watertown, Massachusetts
1	Commanding General U. S. Army Chemical Warfare Laboratories Army Chemical Center, Maryland	1	Applied Physics Lab. 8621 Georgia Avenue Silver Spring, Maryland
1	Director JPL Ord Corps Installation 4800 Oak Grove Drive Department of the Army Pasadena, California Attn: Reports Group	1	Armour Research Foundation Institute of Technology Chicago, Illinois
1	The Johns Hopkins University Operations Research Office 6935 Arlington Road Bethesda 14, Maryland	1	Aerophysics Development Corporation Pacific Palisades California
3	Commanding Officer Picatinny Arsenal Dover, New Jersey	1	ARO, Inc. Tullahoma, Tennessee
2	Commanding General Army Rocket & Guided Missile Agency Redstone Arsenal, Alabama Attn: Technical Library - ORDXR-OTL	1	Aircraft Armament, Inc. Cockeysville, Maryland
1	Commanding General Ordnance Ammunition Command Joliet, Illinois	1	AVCO Manufacturing Co. 20 S. Union Street Lawrence, Massachusetts
1	Commanding General Ordnance Weapons Command Rock Island Arsenal Illinois	1	Aerojet Engineering Co. Azusa, California Attn: Mr. M. T. Grenier Librarian
		1	Boeing Aircraft Company Seattle, Washington
		1	Bell Aircraft Corporation Buffalo New York
		1	Bendix Aviation Corporation South Bend Indiana

# DISTRIBUTION LIST

<u>No. of Copies</u>	<u>Organization</u>	<u>No. of Copies</u>	<u>Organization</u>
1	Bulova Research & Development Laboratories, Inc. 62-10 Woodside Avenue Woodside, New York	1	Eastman Kodak Company Navy Ordnance Division Rochester 14, New York Attn: Dr. Robert Trotter
2	Budd Manufacturing Co. Red Lion and Verree Roads Philadelphia 15, Pa.	2	Firestone Tire and Rubber Company Akron, Ohio
1	Chamberlain Corporation Waterloo Iowa	1	General Electric Co. Missile and Ordnance Systems Department 3198 Chestnut Street Philadelphia, Pa.
1	Chicago Midway Laboratories University of Chicago 6220 S. Drexel Avenue Chicago 37, Illinois	1	General Mills, Inc. Minneapolis 13 Minnesota
1	CONVAIR Division of General Dynamics Corp. P. O. Box 1950 San Diego 12, California Attn: D. H. Bennett, Chief of Aero.	1	Grumman Aircraft Eng. Corporation Bethpage New York
1	Cornell Aeronautical Laboratory 4455 Genessee Street Buffalo, New York Attn: Library	1	M. W. Kellogg Co. Foot of Danforth Avenue Jersey City 3, New Jersey Attn: Mr. Robert A. Miller
1	Consolidated Vultee Aircraft Corp. Ord Aerophysics Laboratory Daingerfield, Texas	1	Johns Hopkins University Institute for Cooperative Research 3506 Greenway Baltimore 18, Maryland Attn: Dr. E. R. C. Miles Project THOR
1	University of Southern California Naval Research Project College of Engineering Los Angeles 7, California Attn: Mr. H. R. Saffell	1	Lockheed Aircraft Corp. Missile Systems Division Sunnyvale, California
1	Douglas Aircraft Company, Inc. 3000 Ocean Park Blvd. Santa Monica, California	1	Marquardt Aircraft Company 7801 Hayvenhurst Avenue Van Nuys, California Attn: Mr. R. E. Marquardt
1	Douglas Aircraft Company, Inc. El Segundo, California		

# DISTRIBUTION LIST

<u>No. of Copies</u>	<u>Organization</u>	<u>No. of Copies</u>	<u>Organization</u>
1	Massachusetts Institute of Technology Cambridge 39 Mass.	1	Ramo-Wooldridge Corp. Guided Missile Research Division P. O. Box 299 Inglewood, California
1	McDonnell Aircraft Corp. P. O. Box 516 St. Louis 3, Missouri	1	University of Texas Defense Research Lab. Austin, Texas Attn: Dr. C. P. Boner
1	North American Aviation, Inc. 12214 Lakewood Boulevard Downey, California	2	United Aircraft Corp. Research Department East Hartford 8, Conn. Attn: Mr. C. H. King Mr. Robert C. Sale
1	Technical Documents Services Willow Run Laboratories University of Michigan Willow Run Airport Ypsilanti, Michigan	1	Wright Aeronautical Corp. Wood-Ridge, New Jersey Attn: Sales Dept. (Govt)
1	The Martin Company Baltimore 3, Maryland	1	North American Aviation, Inc.. Columbus, Ohio
1	Chairman Aeronautical Engineering Dept. Princeton University Princeton, New Jersey	1	Professor J. W. Beams Dept. of Physics University of Virginia Charlottesville, Va.
1	Purdue University Lafayette, Indiana Attn: Dr. M. J. Zucrow	1	Professor Clark B. Millikan Guggenheim Aero. Lab. California Inst. of Tech. Pasadena 4, California
1	Republic Aviation Corporation Military Contract Department Farmingdale, L. I. New York Attn: Dr. William O'Donnell	1	Dr. A. E. Puckett Hughes Aircraft Company Florence Avenue at Teat St. Culver City, California
1	Ryan Aeronautical Company Lindbergh Field San Diego 12, California Attn: Mr. Bruce Smith	1	Office, Technical Services Dept. of Commerce Washington 25, D. C. Attn: Mr. George K. Taylor Chief, Tech Reports Sec.
1	Radiaplane Corporation Metropolitan Airport Van Nuys, California Attn: Mr. Ferried M. Smith		